

1 **A sustained type I IFN-neutrophil-IL-18 axis drives pathology during mucosal viral infection**

2

3 Tania J. Lebratti^{1,§,#}, Ying Shiang Lim^{1,#}, Adjoa Cofie¹, Prabhakar S. Andey², Xiaoping Jiang¹,
4 Jason M. Scott¹, Maria Rita Fabbri^{1,^}, Ayse N. Ozanturk¹, Christine T.N. Pham⁴, Regina A.
5 Clemens³, Maxim Artyomov², Mary C. Dinauer⁵, Haina Shin^{1,*}

6

7 ¹Department of Medicine/Division of Infectious Diseases; ²Department of Pathology and
8 Immunology; ³Department of Pediatrics/Division of Critical Care Medicine; ⁴Department of
9 Medicine/Division of Rheumatology; ⁵Department of Pediatrics/Hematology and Oncology,
10 Washington University School of Medicine, St Louis, MO, USA

11

12 [§]Current address: Bayer, Crop Science Division, St Louis, MO, USA

13 [^]Current address: Department of Molecular and Clinical Cancer Medicine, Northwest Cancer
14 Research Centre, University of Liverpool, Liverpool, UK

15

16 [#]These authors contributed equally.

17 ^{*}Corresponding author: haina.shin@wustl.edu

18

19 Running title: Pathogenic neutrophil responses during HSV-2 infection

20 **ABSTRACT**

21 Neutrophil responses against pathogens must be balanced between protection and
22 immunopathology. Factors that determine these outcomes are not well-understood. In a mouse
23 model of genital herpes simplex virus-2 (HSV-2) infection, which results in severe genital
24 inflammation, antibody-mediated neutrophil depletion reduced disease. Comparative single cell
25 RNA-sequencing analysis of vaginal cells against a model of genital HSV-1 infection, which
26 results in mild inflammation, demonstrated sustained expression of interferon-stimulated genes
27 (ISGs) only after HSV-2 infection primarily within the neutrophil population. Both therapeutic
28 blockade of IFN α / β receptor 1 (IFNAR1) and genetic deletion of IFNAR1 in neutrophils
29 concomitantly decreased HSV-2 genital disease severity and vaginal IL-18 levels. Therapeutic
30 neutralization of IL-18 also diminished genital inflammation, indicating an important role for this
31 cytokine in promoting neutrophil-dependent immunopathology. Our study reveals that sustained
32 type I IFN signaling is a driver of pathogenic neutrophil responses, and identifies IL-18 as a novel
33 component of disease during genital HSV-2 infection.

34

35 INTRODUCTION

36 Neutrophils are a critical component of the innate immune system. In humans, they are
37 the most abundant leukocyte in circulation and are often amongst the first wave of immune cells
38 responding to pathogen invasion. In the context of bacterial or fungal infection, including those
39 that are sexually transmitted, neutrophils are largely protective and can help eliminate pathogens
40 through a variety of effector functions, including phagocytosis, production of reactive oxygen
41 species (ROS), NET and protease release, and cytokine and chemokine secretion (Mayadas,
42 Cullere, & Lowell, 2014; Pham, 2006; Tecchio, Micheletti, & Cassatella, 2014). In contrast, the
43 role of neutrophils during viral infection is less clear (Galani & Andreakos, 2015). While
44 neutrophils have been reported to neutralize several viruses and display protective qualities in vivo
45 (Akk, Springer, & Pham, 2016; Craig N. Jenne et al., 2013; Saitoh et al., 2012; Tate et al., 2009;
46 Tate et al., 2011) they have also been associated with tissue damage, loss of viral control, and
47 increased mortality (Bai et al., 2010; Brandes, Klauschen, Kuchen, & Germain, 2013; Kulkarni et
48 al., 2019; Narasaraju et al., 2011; Vidy et al., 2016).

49 Type I IFNs are potent regulators of neutrophil activity in a multitude of contexts. Type I
50 IFN can enhance recruitment of neutrophils to sites of infection, regulate neutrophil function and
51 drive immunopathology after infection by different classes pathogens, including *Plasmodium spp.*,
52 *Candida spp.* and *Pseudomonas spp.* (Majer et al., 2012; Pylaeva et al., 2019; Rocha et al., 2015).
53 However, type I IFNs can also inhibit neutrophil recruitment to the ganglia by suppressing
54 chemokine expression after HSV infection (Stock, Smith, & Carbone, 2014), suggesting that the
55 interplay of IFNs and neutrophil activity may be dependent on tissue type and the pathogen. The
56 relationship between neutrophil-intrinsic type I IFN signaling and infection outcomes is less clear.
57 Type I IFNs can promote expression of interferon stimulated genes (ISGs) and pro-inflammatory

58 cytokines in neutrophils, suggesting a potential role in driving immunopathology (Galani et al.,
59 2017). During *Leishmania* infection, however, IFNAR signaling appears to suppress neutrophil-
60 dependent killing of parasites (Xin et al., 2010), which emphasizes the complexity of IFN-
61 mediated neutrophil responses.

62 Genital herpes is a chronic, sexually transmitted infection that affects over 400 million
63 people worldwide (World Health Organization, 2007) and can be caused by two members of the
64 alphaherpesvirus family, herpes simplex virus-2 (HSV-2) or the related HSV-1. Genital herpes is
65 characterized by recurrent episodes of inflammation and ulceration and the factors that drive
66 disease are unclear. In humans, ulcer formation is associated with suboptimal viral control and
67 spread during episodes of reactivation (Roychoudhury et al., 2020; J. T. Schiffer & Corey, 2013;
68 Joshua T Schiffer et al., 2013), while in mouse models, severity of disease often correlates with
69 susceptibility to infection and the level of viral replication in the genital mucosa (Gopinath et al.,
70 2018). Neutrophil infiltration into sites of active HSV-2 ulcers have also been reported in humans
71 (Boddingius, Dijkman, Hendriksen, Schiff, & Stolz, 1987), but whether these cells are helpful or
72 harmful during HSV infection is unknown. While neutrophils have been associated with tissue
73 damage after multiple routes of HSV-1 infection (Divito & Hendricks, 2008; Khoury-Hanold et
74 al., 2016; Rao & Suvas, 2018; Thomas, Gangappa, Kanangat, & Rouse, 1997), a protective role
75 for neutrophils after genital HSV-2 infection has also been reported (Milligan, 1999; Milligan,
76 Bourne, & Dudley, 2001), although use of non-specific depletion antibodies have muddled the
77 respective contribution of neutrophils and other innate immune cells such as monocytes, which are
78 known to be antiviral (Iijima, Mattei, & Iwasaki, 2011). Furthermore, increased neutrophil
79 recruitment to the HSV-2 infected vaginal epithelial barrier resulted in greater epithelial cell death,
80 suggesting that neutrophil responses may indeed be pathogenic (Krzyszowska et al., 2014).

81 However, the factors that distinguish pathogenic vs non-pathogenic neutrophil responses during
82 viral infection, including HSV-2 infection, remain ill-defined.

83 To address this, we evaluated the impact of neutrophils on genital disease severity using
84 two models of HSV infection that result in low levels (HSV-1) or high levels of inflammation
85 (HSV-2) (A. G. Lee et al., 2020). Between these two states, heightened expression of type I IFN
86 during the resolution phase of acute infection and sustained expression of ISGs in neutrophils was
87 detected after HSV-2 infection but not HSV-1. Therapeutic antibody-mediated blockade of
88 IFNAR1 as well as neutrophil-specific deletion of IFNAR1 reduced both genital inflammation as
89 well as vaginal IL-18 levels during the resolution phase of acute HSV-2 infection. Accordingly,
90 therapeutic neutralization of IL-18 also ameliorated genital disease after HSV-2 infection.
91 Together, our data demonstrates that sustained type I IFN signaling is a key determinant of
92 pathogenic neutrophil responses during viral infection, and identifies neutrophil- and type I IFN-
93 dependent IL-18 production as a novel driver of inflammation during genital HSV-2 infection.

94 **RESULTS**

95 *Neutrophils are a component of severe genital inflammation after vaginal HSV-2 infection.*

96 To determine the role of neutrophils in our model of vaginal HSV-2 infection, wildtype
97 (WT) female C57BL/6 mice were treated with Depo-Provera (depot medroxyprogesterone, DMPA)
98 to hold mice at the diestrus phase of the estrus cycle and normalize susceptibility to infection
99 (Kaushic, Ashkar, Reid, & Rosenthal, 2003). Neutrophils were depleted in DMPA-treated mice
100 by intraperitoneal (i.p.) injection of an antibody against Ly6G, a neutrophil-specific marker, or an
101 isotype control. One day later, mice were inoculated intravaginally with 5000 plaque forming units
102 (PFU) of WT HSV-2 strain 186 syn+ (WT HSV-2). Neutrophils were effectively depleted from
103 the vagina up to 5 d.p.i. (Figure 1A). In order to focus on genital inflammation, mice were
104 monitored for 1 week after infection, as progression of disease within the second week of our
105 infection model is largely indicative of viral dissemination into the central nervous system. In both
106 cohorts, mild genital inflammation was apparent starting at 4 d.p.i. in a small fraction of mice
107 (Figure 1B). Over time, progression of disease in the neutrophil-depleted mice was significantly
108 slower compared to the controls. Remarkably, as late as 7 d.p.i., a proportion of the neutrophil-
109 depleted group remained uninflamed, in contrast to the isotype control group in which all mice
110 displayed signs of inflammation (Figure 1B). To confirm the disparity in scored disease severity,
111 we examined the vagina and genital skin by histology. At 6 d.p.i., epithelial denuding and damage
112 was apparent in the isotype control-treated mice (Figure 1C). In contrast, only a limited amount of
113 epithelial destruction was observed in neutrophil-depleted mice, with less cellular infiltrates at
114 sites of damage and in the lumen (Figure 1C). Furthermore, the epithelial layer proximal to areas
115 of damage was morphologically distinct in isotype control-treated animals compared to neutrophil-
116 depleted animals, suggesting diverse epithelial responses after infection in the presence or absence

117 of neutrophils (Figure 1C). Similarly, destruction of the epidermis and separation of the epidermis
118 from the dermis was widespread in the genital skin of isotype control-treated mice but not in
119 neutrophil-depleted mice (Figure 1C). Unexpectedly, differences in genital inflammation and
120 mucosal damage were largely independent of changes in viral control in the absence of neutrophils,
121 as viral shedding into the vaginal lumen was similar between the two groups (Figure 1D). Indeed,
122 disease severity was decreased in neutrophil-depleted mice despite a slight delay in the resolution
123 of viral replication at 5 d.p.i. (Figure 1D).

124 We next evaluated whether the decreased inflammation after neutrophil depletion was due
125 to changes in the cellular response against HSV-2 infection. We examined the recruitment of
126 Ly6C⁺ monocytes, NK cells, CD4 and CD8 T cells, all of which have been implicated in either
127 the control of HSV or modulation of disease severity (A. J. Lee & Ashkar, 2012; Shin & Iwasaki,
128 2013; Truong, Smith, Sandgren, & Cunningham, 2019). To remove intravascular cells and to limit
129 our analysis to cells within the vagina, tissues were thoroughly perfused prior to collection (Scott
130 et al., 2018). Unexpectedly, there was no significant difference in the number of Ly6C⁺CD11b⁺
131 cells (Figure 1 - Supplement 1A), NK cells (Figure 1 - Supplement 1B), total CD4 (Figure 1 -
132 Supplement 1C) or CD8 T cells (Figure 1 - Supplement 1D) that were recruited to the vagina over
133 the first six days after infection regardless of whether neutrophils were present or not. Thus, our
134 data demonstrate that neutrophils do not play a significant antiviral role in our model of vaginal
135 HSV-2 infection, and rather promote genital inflammation with minimal impact viral burden and
136 recruitment of other immune cells to the vagina.

137

138 *Neutrophil extracellular trap formation and oxidative burst are not major drivers of genital*
139 *inflammation after HSV-2 infection.*

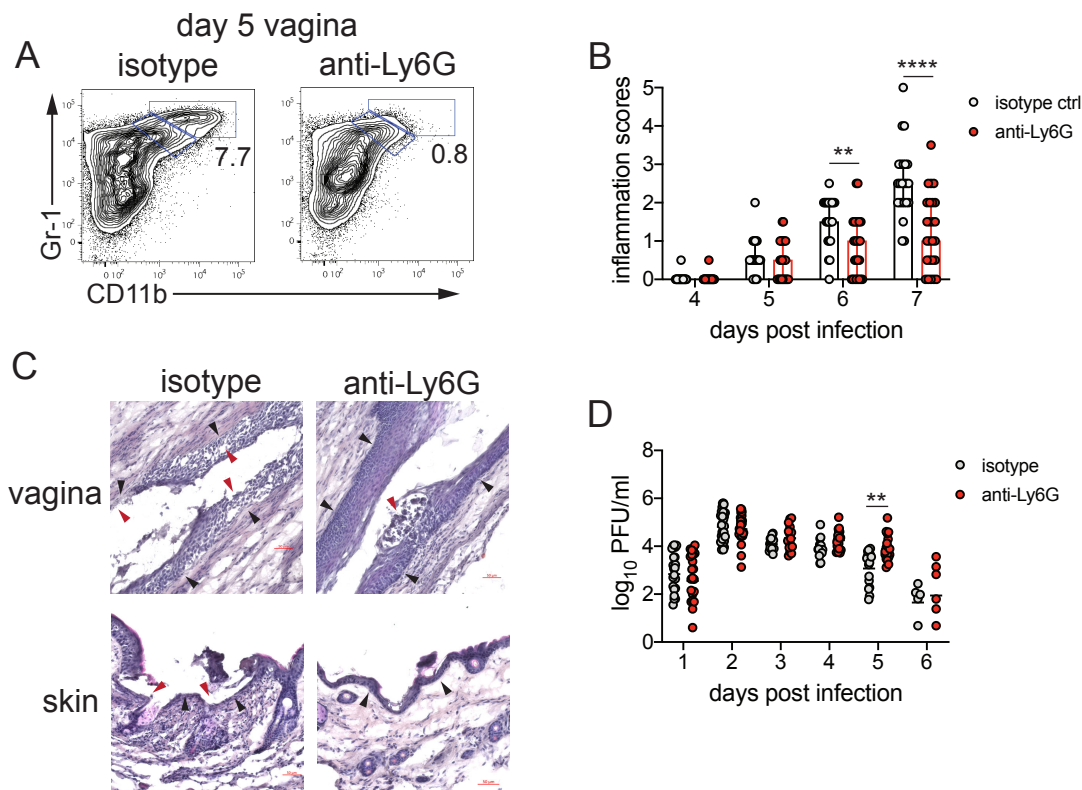


Figure 1. Neutrophil depletion reduces disease severity after HSV-2 vaginal infection. Female C57BL/6J mice were treated with DMPA and inoculated intravaginally (ivag) with 5000 PFU HSV-2. One day prior to HSV-2 inoculation, mice were injected intraperitoneally (i.p.) with 500 μ g of rat IgG2a isotype control or anti-Ly6G. **A.** Depletion was confirmed by flow cytometry in the vagina at 5 d.p.i.. Numbers in plots show the frequency of Gr-1+ CD11b+ neutrophils. **B.** Inflammation scores over the first 7.d.p.i. of mice treated with anti-Ly6G antibody (n=25) or isotype control (n=23) Mice showed no signs of disease prior to 4 d.p.i. **C.** Histology of the vagina (top) or genital skin (bottom) at 6 d.p.i. from isotype control (left) or anti-Ly6G antibody-treated mice (right). Red arrows point to areas of epithelial denuding or damage, black arrows denote the basement membrane. **D.** Infectious virus as measured by plaque assay in vaginal washes collected daily (both groups day 1: n=22, day 2: n=28, day 3: n=15, day 4: n=16, day 5: n=19, day 6: n=6). Data in **B** and **D** are pooled from 4 independent experiments. Data in **C** is representative of 2 independent experiments. Bars in **B** show median with interquartile range. Horizontal bars in **C** show mean. Statistical analysis was performed by repeated measures two-way ANOVA with Geisser-Greenhouse correction and Bonferroni's multiple comparisons test (**B**) or repeated measures two-way ANOVA with Bonferroni's multiple comparison's test (**D**). **p<0.01, ****p<0.001. Raw values for each biological replicate, epsilon values and specific p values are provided in Figure 1 - Source Data.

140 We next wanted to determine whether neutrophil-specific effector functions were
141 promoting disease after HSV-2 infection. NETs have been associated with tissue damage in the
142 context of both infectious (C. N. Jenne & Kubes, 2015) and non-infectious disease (Granger,
143 Peyneau, Chollet-Martin, & de Chaisemartin, 2019). To test whether NETs play a role in genital
144 disease after HSV-2 infection, we first examined the ability of neutrophils to form NETs when
145 exposed to HSV-2. *In vitro* stimulation of neutrophils with HSV-2 resulted the enlargement of cell
146 nuclei and the characteristic expulsion of DNA coated in citrullinated histones, which is a key
147 characteristic of NETs (Figure 1 - Supplement 2A). The formation of NETs requires input from
148 multiple pathways, including histone citrullination by enzymes such as PAD4, which leads to
149 chromatin de-condensation and the eventual release of DNA (P. Li et al., 2010). To generate
150 animals that were specifically lacking PAD4 in neutrophils, we bred PAD4^{fl/fl} x MRP8-Cre mice
151 (PAD4 CKO). HSV-2 infection of these mice and their littermate controls demonstrated minimal
152 impact on genital inflammation (Figure 1 - Supplement 2B) or viral replication (Figure 1 -
153 Supplement 2C) in the genital mucosa. Thus, our data show PAD4 expression in neutrophils, and
154 likely NET formation, are not the mechanisms by which these cells mediate disease after HSV-2
155 infection.

156 We next tested whether ROS production by neutrophils mediated inflammation after HSV-
157 2 infection. While production of ROS in neutrophils supports antimicrobial activity against a
158 variety of pathogens (Dinauer, 2019), excessive oxidative stress can be associated with tissue
159 injury (Mittal, Siddiqui, Tran, Reddy, & Malik, 2014). We found that *in vitro* stimulation of
160 neutrophils with HSV-2 led to an increase in ROS production compared to unstimulated cells
161 (Figure 1 - Supplement 3A). To determine whether respiratory burst in neutrophils promoted
162 genital inflammation after HSV-2 infection *in vivo*, we infected mice with germline deficiency in

163 Ncf2 (Ncf2 KO), which encodes p67^{phox}, a key component of the NADPH oxidase complex (Jacob
164 et al., 2017). HSV-2 infection of Ncf2 KO and heterozygous controls resulted in similar
165 progression of disease (Figure 1 - Supplement 3B) and did not alter viral titer (Figure 1 -
166 Supplement 3C). To confirm that tested neutrophil effector functions, including ROS production,
167 we infected mice in which the calcium-sensing molecules STIM1 and STIM2 were deleted from
168 neutrophils (Clemens, Chong, Grimes, Hu, & Lowell, 2017). Stim1^{fl/fl} x Stim2^{fl/fl} x MRP8-Cre
169 (STIM1/2 DKO) mice were infected with HSV-2 and monitored for disease. As expected, there
170 was little difference in genital inflammation severity between the STIM1/2 DKO and Cre- controls
171 (Figure 1- Supplement 3D) or viral titers (Figure 1 - Supplement 3E). Together, our data show that
172 ROS production from neutrophils and other cell types play little role in driving genital
173 inflammation after HSV-2 infection.

174

175 ***A type I IFN signature distinguishes neutrophil responses after genital HSV-1 and HSV-2***
176 ***infection.***

177 To identify the factors that drove pathogenic neutrophil responses after HSV-2 infection,
178 we turned to a complementary model of HSV-1 genital infection that we had previously described
179 (A. G. Lee et al., 2020). Inoculation with the same dose of HSV-1 and HSV-2 led to profound
180 differences in genital inflammation (Figure 2A) despite comparable levels of mucosal viral
181 shedding (A. G. Lee et al., 2020). Importantly, magnitude of the neutrophil response in the vagina
182 was similar between HSV-1 and HSV-2 infected mice during the course of acute mucosal infection
183 (Figure 2B), and neutrophils could be found infiltrating sites of both HSV-1 and HSV-2-infected
184 epithelium, although it appeared that the interaction between neutrophil and virally infected
185 epithelial cells after HSV-1 inoculation was not as extensive as after HSV-2 inoculation (Figure

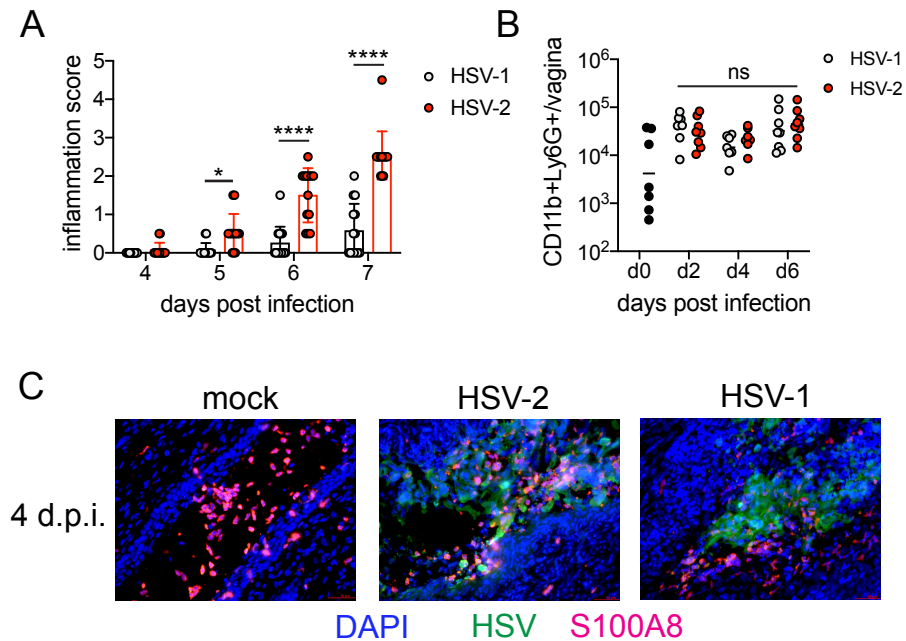


Figure 2. Magnitude of the neutrophil response during HSV-1 and HSV-2 is similar despite difference in disease outcome. Female C57BL/6J mice were treated with DMPA and inoculated ivag with 10^4 PFU HSV-1 McKrae or HSV-2. **A**. Inflammation scores were monitored for 7 d.p.i.. For HSV-1: n=14, HSV-2: n=13. **B**. Neutrophils were counted by flow cytometry in vaginal tissues at the indicated days after HSV-1 or HSV-2 infection. For d0: n=7, day 2: n=8, day 4: n=7, day 6: n=8. **C**. Vaginas were harvested from PBS inoculated (mock), HSV-1 or HSV-2 inoculated mice at 4 d.p.i., and tissue sections were probed with antibodies against HSV proteins (green) or S100A8 (red). DAPI (blue) was used to detect cell nuclei. Images are representative of six mice per group. Data are pooled from 3 (**A**) or 2 (**B**, **C**) independent experiments. Bars show median with interquartile range in **A** and mean in **B**. Statistical significance was measured by repeated measures two-way ANOVA with Geisser-Greenhouse correction and Bonferroni's multiple comparisons test (**A**) or two-way ANOVA with Bonferroni's multiple comparisons test (**B**). * $p < 0.05$, **** $p < 0.001$, ns = not significant. Raw values for each biological replicate, epsilon values and specific p values are provided in Figure 2 - Source Data.

186 2C). In contrast to HSV-2 infection, antibody-mediated depletion of neutrophils with anti-Ly6G
187 antibody prior to inoculation with HSV-1 did not reduce the development of genital inflammation
188 during the first 7 days after infection (Figure 2 - Supplement 1). Together, our data suggests that
189 the regulation of the neutrophil response after HSV-1 or HSV-2 infection was distinct, leading to
190 disparate inflammatory outcomes.

191 To better understand the differences between pathogenic neutrophil responses after
192 HSV-2 infection and the non-pathogenic neutrophil responses after HSV-1, we performed single
193 cell RNA-sequencing (scRNA-seq) on sorted live vaginal cells from a mock infected mouse or
194 mice infected with HSV-1 or HSV-2 using the 10x Genomics platform (Zheng et al., 2017). Each
195 sample was comprised of cells from a single animal in to better delineate potential subsets within
196 cell populations, particularly neutrophils. Analysis across 21,633 cells in all samples revealed 17
197 unique clusters in the vagina during HSV infection after filtering, including myeloid cells,
198 lymphocytes and epithelial cells (Figure 3A). Neutrophils were identified by expression of known
199 cell markers such as *S100a8* and *Csf3r* (Figure 3B). In mock infected animals, the vaginal
200 neutrophil population was dominated by cluster 0, and upon infection, at least two additional
201 neutrophil subsets, cluster 2 and cluster 5, were clearly present (Figure 3C). While HSV-1 infected
202 mice retained all three subpopulations of neutrophils in the vagina at 5 d.p.i., in HSV-2 infected
203 mice the presence of cluster 0 was greatly reduced and the bulk of the neutrophils was composed
204 of cluster 2 and 5 (Figure 3C). One major distinguishing characteristic between "homeostatic"
205 cluster 0 and "infection" clusters 2 and 5 was the extent of ISG expression, in which cluster 0
206 expressed low levels of genes associated with a type I IFN response, even in infected animals,
207 while clusters 2 and 5 expressed high levels of these genes (Figure 3D) (Liberzon et al., 2015).
208 Furthermore, expression of ISGs within clusters 2 and 5 was higher after HSV-2 infection

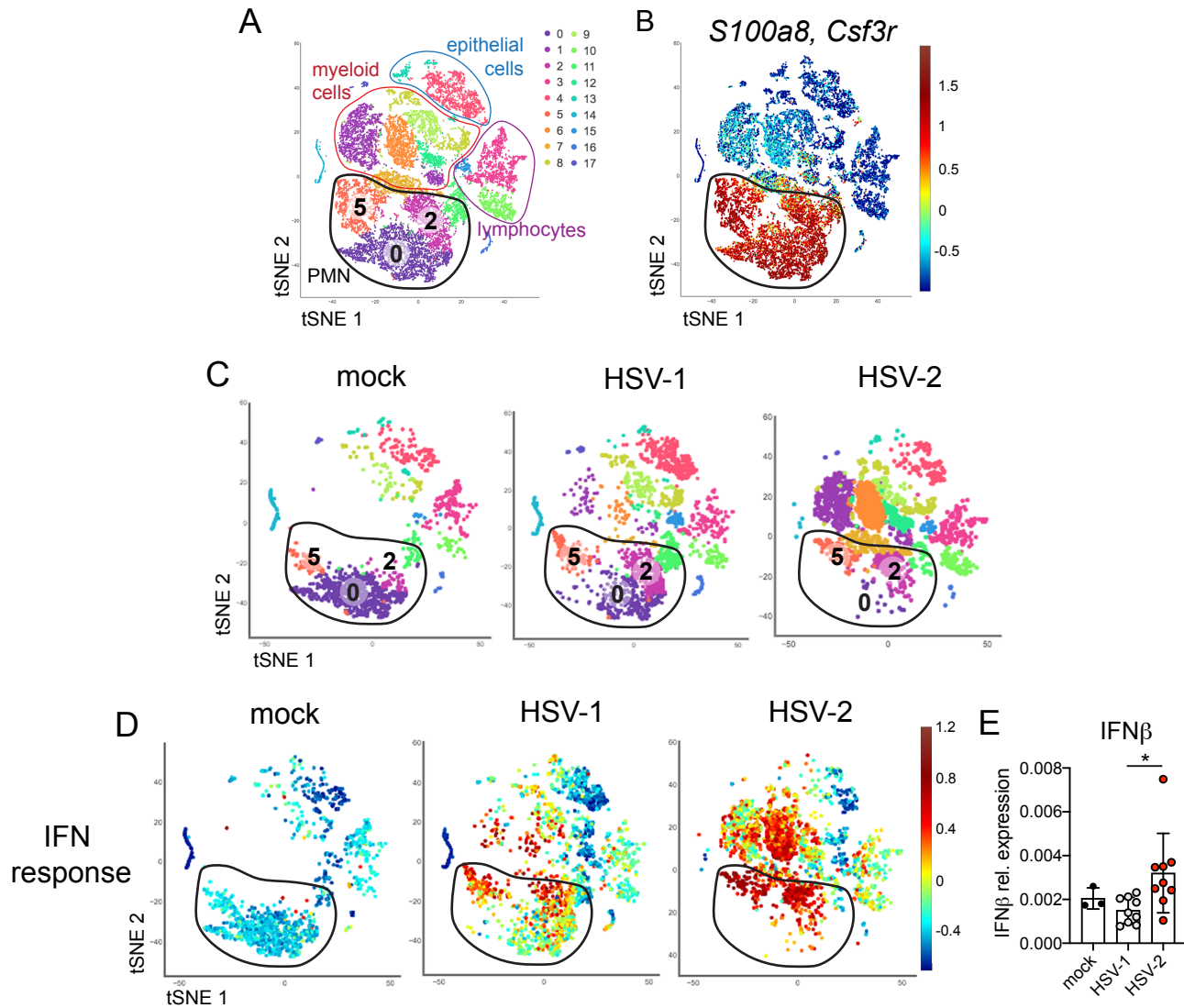


Figure 3. Single cell transcriptome analysis reveals a sustained IFN signature in the neutrophil response against HSV-2. Mice were infected as described in Figure 2. Vaginas were harvested at 5 d.p.i., live cells were flow sorted and subjected to high-throughput scRNA-seq. **A.** A t-Distributed Stochastic Neighbor Embedding (tSNE) visualization of 21,633 cells across all mice resolves 17 distinct clusters in the vaginal tissue. Clusters can be identified as myeloid cells (red border), epithelial cells (blue border) or lymphocytes (purple border). Neutrophils are encircled in black, and contain three distinct clusters (0, 2 and 5). **B.** Neutrophils are defined by high expression of *S100A8* and *G-CSFR* (*Csf3r*). **C.** tSNE plots of vaginal cell clusters from mock inoculated or HSV-1 or HSV-2 infected mice. Neutrophil populations are circled in black. **D.** Distribution of expression for genes within the Hallmark IFN α Response gene set. **E.** Expression of IFN β transcripts normalized to RPL13 in mock inoculated (n=3) mice or mice at 5 d.p.i. with HSV-1 (n=9) or HSV-2 (n=9) as measured by qRT-PCR. scRNA-seq in **A-D** was performed once. Data in **E** are pooled from 2 independent experiments. Statistical significance was measured by one-way ANOVA with Tukey's multiple comparisons test. *p<0.05. Raw values for each biological replicate and specific p values for **E** are provided in Figure 3 - Source Data.

209 compared to HSV-1 (Figure 3C), which was confirmed by quantitative RT-PCR (qRT-PCR)
210 analysis of select ISGs that are differentially expressed in the vagina at 5 days after HSV-1 or
211 HSV-2 infection (Figure 3 - Supplement 1). qRT-PCR shows that expression of CXCL10 (Figure
212 3 - Supplement 1A, B) and Gbp2 (Figure 3 - Supplement 1C, D) is increased in HSV-2 infected
213 vaginas compared to HSV-1, while IL-15 is not (Figure 3 - Supplement 1E, F), which supports the
214 accompanying scRNA-seq analysis. While type I IFN was robustly produced early during acute
215 infection after both HSV-1 and HSV-2 infection (Figure 3 - Supplement 2), greater expression of
216 IFN β was detected in the vagina after HSV-2 infection compared to HSV-1 at time points
217 corresponding to the onset of genital inflammation (Figure 3E). Thus, during viral infection,
218 distinct neutrophil subsets can be classified by transcriptional profiling, and expression of ISGs
219 suggest that a key difference between a pathogenic and non-pathogenic neutrophil response during
220 viral infection may be sustained IFN signaling.

221

222 ***Sustained cell-intrinsic type I IFN signaling is required for pathogenic neutrophil responses***
223 ***during HSV-2 infection.***

224 We next wanted to test whether type I IFN signaling promoted immunopathology during
225 genital HSV-2 infection. IFNAR1-deficient mice are highly susceptible to HSV regardless of the
226 route of inoculation (Gill, Deacon, Lichty, Mossman, & Ashkar, 2006; Iversen, Ank, Melchjorsen,
227 & Paludan, 2010; Iversen et al., 2016; Reinert et al., 2012; Royer et al., 2019; Svensson, Bellner,
228 Magnusson, & Eriksson, 2007; Wilcox, Folmsbee, Muller, & Longnecker, 2016), and rapidly
229 succumb to infection, mainly due to a loss of viral control. To investigate the temporal effects of
230 type I IFNs in HSV-2 genital disease, we used an antibody against IFNAR1 to block the receptor
231 at different time points after infection (Scott et al., 2018). When mice were injected i.p. with anti-

232 IFNAR1 antibody on the day of HSV-2 inoculation, disease progression was more rapid compared
233 to isotype control treated animals (Figure 4 - Supplement 1A), and mice succumbed to infection
234 at a faster rate (Figure 4 - Supplement 1B), in a manner similar to IFNAR1-deficient mice (Iversen
235 et al., 2010; Iversen et al., 2016; A. J. Lee et al., 2017; Reinert et al., 2012; Wang et al., 2012).
236 Inflammation and rapid disease progression were likely due to significantly elevated viral burden
237 in the anti-IFNAR1 antibody treated mice compared to isotype controls (Figure 4 - Supplement
238 1C), as HSV is a highly lytic virus that is capable of independently inducing epithelial tissue
239 damage (Horbul, Schmechel, Miller, Rice, & Southern, 2011). To focus on the effects of persistent
240 IFN signaling in the vagina after HSV-2 infection, we also treated mice with a single injection of
241 anti-IFNAR1 antibody or an isotype control at 4 d.p.i.. In stark contrast to early anti-IFNAR1
242 antibody treatment, one treatment with therapeutic IFNAR1 blockade led to a significant reduction
243 in the severity of inflammation compared to isotype controls (Figure 4A). Histology of vaginal
244 tissues from isotype-treated controls at 6 d.p.i. showed widespread epithelial denuding and
245 immune cell infiltrates within the epithelial layer of the vagina (Figure 4B). In contrast, damage to
246 the vaginal epithelium in anti-IFNAR1 antibody-treated mice appeared to be localized (Figure 4B),
247 similar to neutrophil-depleted mice (Figure 1C). Similarly, the genital skin of isotype control-
248 treated mice displayed signs of severe inflammation and destruction of the epidermis, while the
249 skin structure of anti-IFNAR1 antibody-treated mice was largely intact (Figure 4B). Furthermore,
250 IFNAR1 blockade at 4 d.p.i. had little impact on mucosal viral shedding (Figure 4C). Collectively,
251 these data show that the protective effect of type I IFN on control of genital HSV infection is
252 limited to the early stages of acute infection, and that sustained IFN signaling in the later stages of
253 acute HSV-2 genital infection drive inflammation with minimal effect on viral replication.

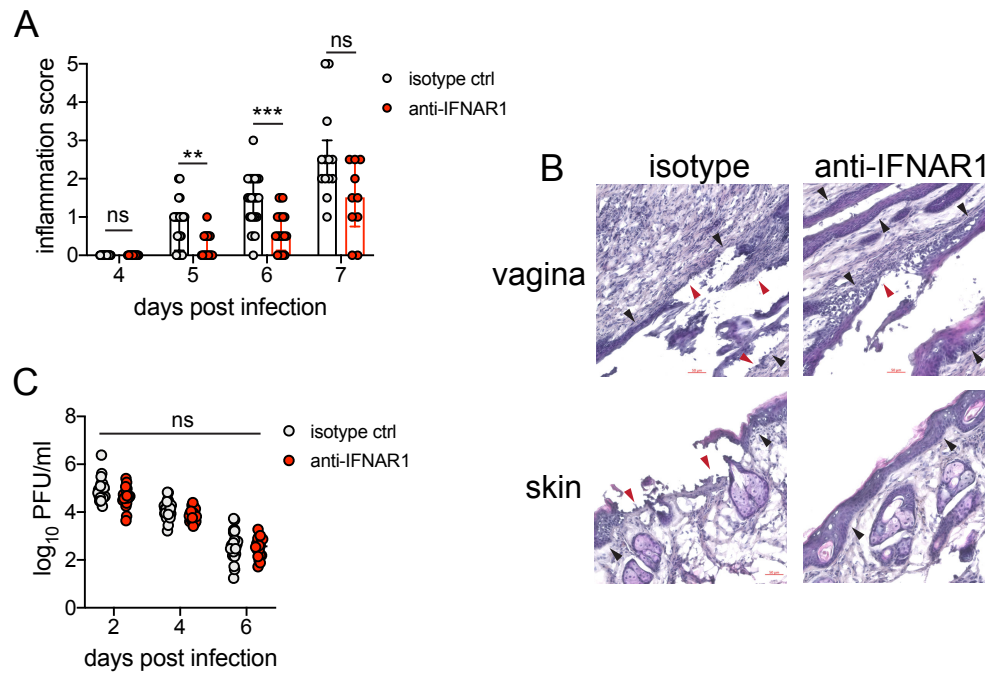


Figure 4. Inhibition of type I IFN signaling during the resolution phase of infection reduces inflammation after HSV-2 infection. Mice were infected as described in Figure 2. At 4 d.p.i., mice were injected i.p. with either 1mg of anti-IFNAR1 antibody (n=10-13) or isotype control (n=7-9) and monitored for disease progression. Mice showing overt signs of genital inflammation at the time of antibody injection (4 d.p.i.) were excluded from the study. **A.** Inflammation scores of antibody-treated mice over the first 7 d.p.i. **B.** Histology of the vagina (top) or genital skin (bottom) at 6 d.p.i. Red arrows point to areas of epithelial denuding or damage. Black areas denote the basement membrane. **C.** Infectious virus as measured by plaque assay in vaginal washes collected on the indicated days. Data are pooled from (A, C) or representative of 3 independent experiments. Bars in A show median with interquartile range, bars in C show mean. Statistical significance was measured by repeated measures two-way ANOVA with Geisser-Greenhouse correction and Bonferroni's multiple comparisons test (A) or two-way ANOVA with Bonferroni's multiple comparisons test (C). *p<0.05, **p<0.01, ***p<0.005, ns = not significant. Raw values for each biological replicate, epsilon values and specific p values are provided in Figure 4 - Source Data.

254 Single-cell transcriptional profiling data suggested that type I IFN signaling was highly
255 robust in vaginal neutrophils after HSV-2 infection (Figure 3D). To determine whether intrinsic
256 IFN signaling in neutrophils promoted immunopathology, we deleted the type I IFN receptor from
257 granulocytes by breeding IFNAR1^{fl/fl} x MRP8-Cre mice (IFNAR1 CKO). After confirming that
258 IFNAR1 ablation was limited to the neutrophil population (Figure 5A), IFNAR1 CKO mice and
259 littermate Cre- controls were vaginally infected with HSV-2. Despite differences in IFNAR1
260 expression, the number of neutrophils recovered from the vaginal lumen was similar between the
261 IFNAR1 CKO mice and their Cre- control littermates (Figure 5B). Strikingly, although the
262 magnitude of the vaginal neutrophil response was similar, we found that the severity of genital
263 inflammation presented by the IFNAR1 CKO mice was significantly reduced compared to the Cre-
264 controls (Figure 5C). As observed after neutrophil depletion, a subset of the IFNAR1 CKO cohort
265 did not develop any signs of inflammation as late as 7 d.p.i. (Figure 5C). Similar to our
266 observations with therapeutic IFNAR1 blockade, IFNAR1 CKO mice exhibited less pathology in
267 both the vagina and genital skin compared to Cre- controls. (Figure 5D). Distinct disease outcomes
268 between the Cre- controls and IFNAR1 CKO mice occurred independently of viral control, as viral
269 load in the mucosa were similar between the two groups (Figure 5E). Together, our data
270 demonstrates that tissue inflammation during HSV-2 infection is largely driven by prolonged type
271 I IFN production, which acts directly upon neutrophils to drive disease.

272

273 ***Sustained type I IFN signaling and neutrophils regulate production of pathogenic IL-18 in the***
274 ***vagina during HSV-2 infection.***

275 Type I IFN stimulation of neutrophils can upregulate ISGs as well as several pro-
276 inflammatory cytokines (Galani et al., 2017). To determine whether type I IFN was driving disease

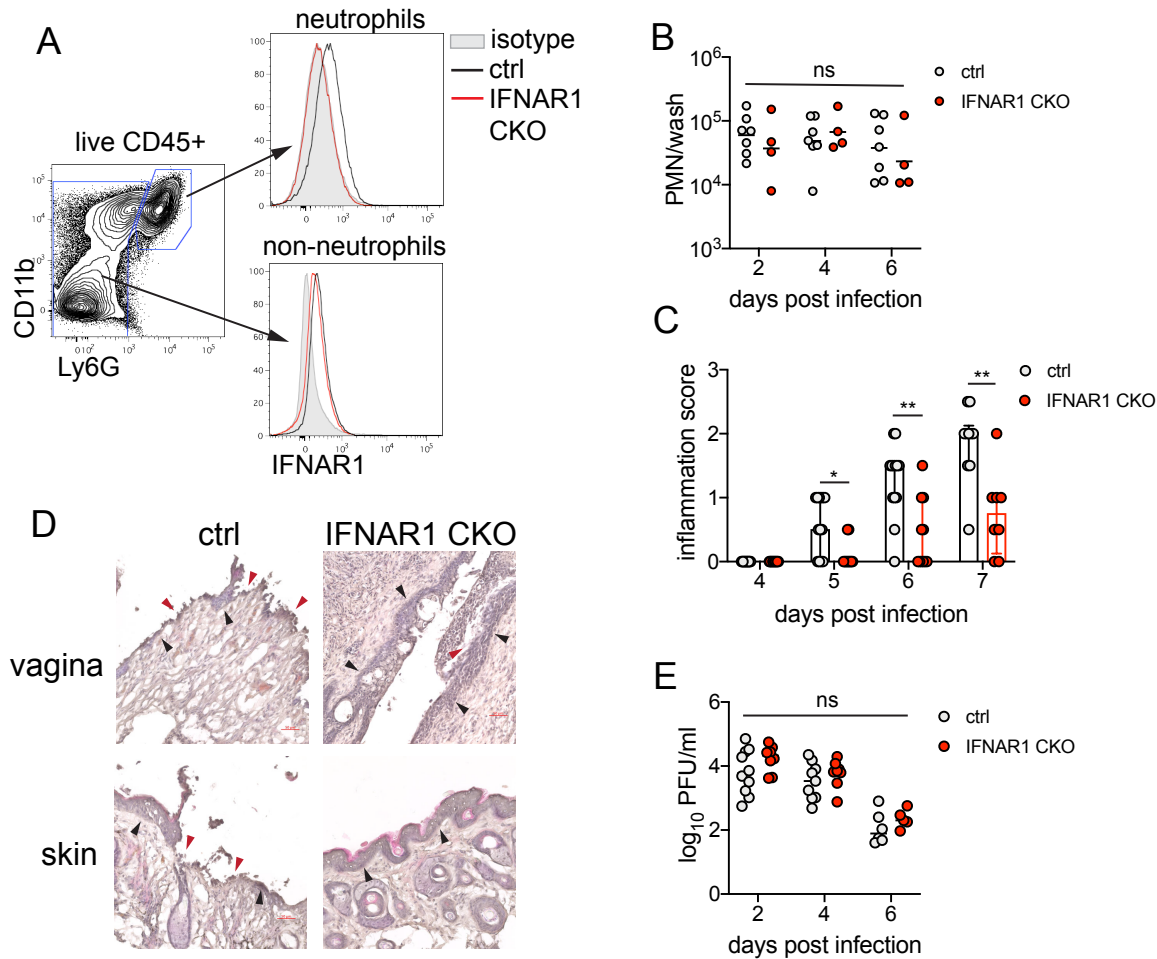


Figure 5. Type I IFN signaling in neutrophils promotes genital inflammation after HSV-2 infection. **A.** IFNAR1 expression on neutrophils and non-neutrophil hematopoietic cells from the bone marrow of naive IFNAR1^{fl/fl} x MRP8-Cre (IFNAR1 CKO) or Cre-littermate controls. Plot is gated on live CD45⁺ cells. CD11b⁺Ly6G⁺ cells are neutrophils, Ly6G⁻ cells are non-neutrophils. Gray histogram shows isotype staining, black open histogram is Cre-control, and red open histogram is IFNAR1 CKO. **B.** Neutrophils were counted by flow cytometry in vaginal washes collected at the indicated days from IFNAR1 CKO (n=4) or Cre-controls (n=7) that were infected with HSV-2 as described in Figure 1. **C.** Inflammation scores for the first 7 d.p.i. of IFNAR1 CKO (n=10-13) or Cre-controls (n=8-11). **D.** Histology on vagina and genital skin at 6 d.p.i.. Red arrows point to areas of epithelial denuding or damage, black arrows denote basement membrane. **E.** Infectious virus as measured by plaque assay from vaginal washes collected on the indicated days from IFNAR1 CKO (n=5-8) or Cre-controls (n=7-10). Data in **C** and **E** are pooled from 3 independent experiments, data in **B** are pooled from 2 independent experiments, and data in **D** are representative of 2 independent experiments. Bars in **C** show median with interquartile range, bars in **B** and **E** show mean. Statistical significance was measured by mixed-effects analysis with (C) or without (B, E) Geisser-Greenhouse correction and Bonferroni's multiple comparisons test. *p < 0.05, **p < 0.01, ns = not significant. Raw values for each biological replicate, epsilon values and specific p values are provided in Figure 2 - Source Data.

277 by shaping the cytokine milieu within the vagina, we first measured several pro-inflammatory
278 cytokines in the vagina at 5 d.p.i., in the presence or absence of neutrophils. The production of
279 inflammatory cytokines such as IL-6 (Figure 6 - Supplement 1A), IL-1 β (Figure 6 - Supplement
280 1B) or TNF (Figure 6 - Supplement 1C), all of which have been associated with genital
281 inflammation and HSV-2 infection in humans (Gosmann et al., 2017; Masson et al., 2014; Murphy
282 & Mitchell, 2016), was similar between both neutrophil-depleted and control groups. Production
283 of IFN γ (Figure 6 - Supplement 1D) as well as IL-12p70 (Figure 6 - Supplement 1E), both
284 cytokines associated with a type I immune response and important for HSV control, were similar
285 between the neutrophil-depleted and control groups. However, when we measured IL-18, an IL-1
286 family cytokine that primarily known for mediating innate defense (Harandi, Svennerholm,
287 Holmgren, & Eriksson, 2001) and for promoting IFN γ production from NK cells during genital
288 HSV-2 infection (A. J. Lee et al., 2017), we detected a notable difference between neutrophil-
289 depleted and control mice (Figure 6A), suggesting an unexpected role for this cytokine in driving
290 disease during HSV-2 infection.

291 To determine whether type I IFN signaling regulated IL-18 production in the vagina, we
292 assessed IL-18 levels in the vaginal lumen after therapeutic antibody-mediated IFNAR1 blockade.
293 At 5 d.p.i., similarly to neutrophil-depleted mice, we found that IL-18 levels were markedly
294 reduced (Figure 6B). Importantly, measurement of IL-18 in the vagina of IFNAR1 CKO at 5 d.p.i.
295 also revealed a significant decrease in cytokine levels compared to littermate controls (Figure 6C).
296 To determine whether IL-18 was playing a key role in driving immunopathology during genital
297 HSV-2 infection, we therapeutically administered an IL-18 neutralizing antibody to HSV-2
298 infected animals starting at 3 d.p.i.. Remarkably, neutralization of IL-18 led to a considerable
299 reduction in disease severity (Figure 6D), without any impact on viral control (Figure 6E). To

300 determine the source of pathogenic IL-18 in the vagina, we probed vaginal tissues for the
301 neutrophil marker S100A8 and IL-18 at 6 d.p.i. (Figure 6F). Detection of IL-18 and S100A8
302 around a single nucleus demonstrated that neutrophils could be a source of IL-18 during vaginal
303 HSV-2 infection (Figure 6F). However, we also identified IL-18-reactive cells that were negative
304 for S100A8 but in close proximity to neutrophils (Figure 6F), suggesting the potential for multiple
305 cellular sources of IL-18. Thus, our data demonstrate that sustained type I IFN signaling in
306 neutrophils leads to the production of vaginal IL-18, and reveal IL-18 to be a novel regulator of
307 disease after HSV-2 infection.

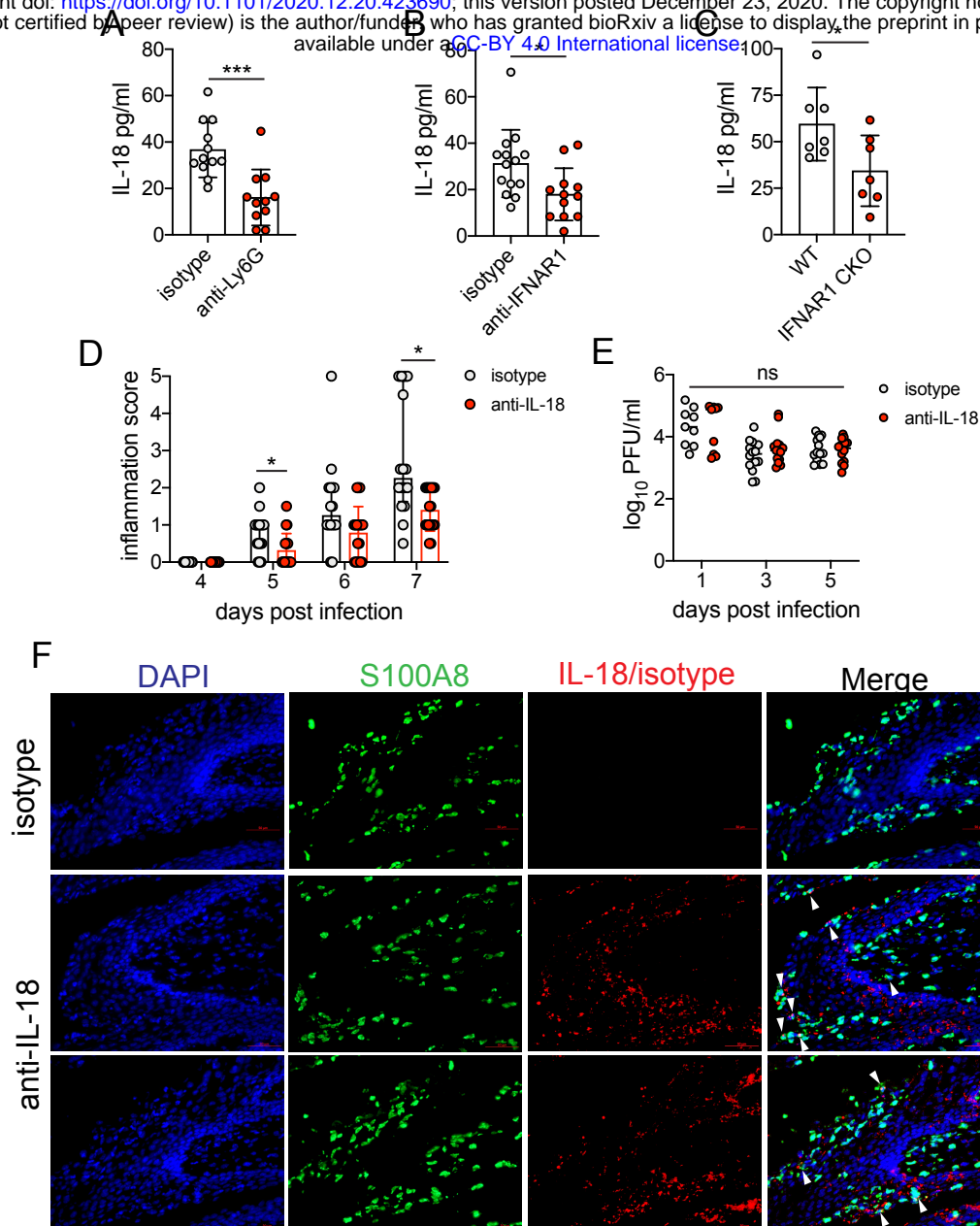


Figure 6. Sustained type I IFN signaling and neutrophils regulate pathogenic IL-18 levels in the vagina. C57BL/6 mice were treated with anti-Ly6G (n=11) or isotype control (n=12) as described in Figure 1 (A), therapeutically treated with anti-IFNAR1 (n=12) or isotype control (n=14) as described in Figure 5 (B) and infected with HSV-2, or IFNAR1 CKO (n=7) and Cre- controls (n=7) were infected with HSV-2 as described in Figure 5 (C). **A-C.** Vaginal IL-18 levels were measured by ELISA in washes collected at 5 d.p.i.. 100µg of anti-IL-18 neutralizing antibody (n=18) or isotype control (n=16) was administered ivag at 3, 4 and 5 d.p.i.. **D.** Inflammation scores of antibody-treated mice over the first 7 d.p.i.. **E.** Infectious virus as measured by plaque assay in vaginal washes collected on the indicated days (n=9-14). **F.** Immunofluorescent staining of vaginal tissues collected at 6 d.p.i.. Green shows S100A8 (neutrophil), red shows IL-18 or isotype, blue is DAPI. Top row shows tissues probed with isotype control, and bottom two rows show two representative images of tissues probed with anti-IL-18 antibody. White arrows point to IL-18+ neutrophils. Data in **A-C**, **D** and **E** are pooled from 4 independent experiments for each experimental setup. Data in **F** is representative of 2 independent experiments. Bars in **A-C** show mean and SD, bars in **D** show median with interquartile range, and bars in **E** show mean. Statistical significance was measured by unpaired t-test (**A-C**), repeated measures two-way ANOVA with (D) Geisser-Greenhouse correction and Bonferroni's multiple comparisons test, or mixed-effects analysis with Bonferroni's multiple comparisons test (**D**). *p<0.05, ***p<0.005, ns = not significant. Raw values for each biological replicate, epsilon values and specific p values are provided in Figure 2 - Source Data.

308 **DISCUSSION**

309 In this study, we evaluated drivers of a pathogenic neutrophil response using a mouse
310 model for an important human infection. We found that neutrophils promote genital inflammation
311 and do not impact antiviral activity after genital HSV-2 infection, suggesting that the neutrophil
312 response is primarily immunopathogenic. Depletion of neutrophils led to a significant decrease in
313 disease severity without affecting recruitment of other immune cells or the production of common
314 pro-inflammatory cytokines, and deficiency in genes controlling neutrophil effector functions such
315 as ROS production and NET formation had little impact on progression of disease. Comparative
316 analysis of single-cell transcriptional profiles revealed a strong type I IFN signature that was
317 sustained in neutrophils responding to a highly inflammatory genital HSV-2 infection but not a
318 less inflammatory HSV-1 infection. In contrast to antibody-mediated blockade of IFNAR1 at the
319 time of infection, which led to significantly worse disease outcomes, IFNAR1 blockade just prior
320 to the resolution phase of acute mucosal infection significantly delayed the progression of genital
321 inflammation. Importantly, neutrophil-specific deficiency of IFNAR1 markedly reduced the
322 severity of genital disease after HSV-2 infection, suggesting that persistent IFN signaling drove
323 disease primary by acting on neutrophils. Ultimately, this sustained type I IFN signaling in
324 neutrophils promoted the production of pro-inflammatory IL-18, and therapeutic neutralization of
325 this cytokine also ameliorated disease. Together, our results suggest an axis of type I IFNs,
326 neutrophils, and IL-18 as key drivers of genital disease in a mouse model of HSV-2 infection, and
327 that sustained type I IFN signaling is a key factor in distinguishing between pathogenic and non-
328 pathogenic neutrophil responses during mucosal viral infection.

329 Type I IFNs are a frontline of defense against viral infection, but models of chronic viral
330 infection, including lymphocytic choriomeningitis virus (LCMV) (Teijaro et al., 2013; Wilson et

331 al., 2013), human immunodeficiency virus (HIV) (Meier et al., 2009; Rotger et al., 2010; Sedaghat
332 et al., 2008; Taleb et al., 2017) and simian immunodeficiency virus (SIV) (Harris et al., 2010;
333 Jacquelin et al., 2009), reveal the detrimental effect of overexuberant or sustained type I IFN
334 signaling. Notably, prolonged IFN signaling during chronic viral infection can promote
335 immunosuppression through multiple cellular and molecular mechanisms, and deletion or
336 blockade of IFNAR1 during chronic LCMV infection can alleviate immunosuppression and
337 enhance long-term viral control (Cheng et al., 2017; Taleb et al., 2017; Teijaro et al., 2013; Wilson
338 et al., 2013). However, unlike the LCMV model, early blockade of type I IFN signaling led to
339 more severe disease and a complete loss of viral control after HSV-2 infection, similar to infections
340 performed on an IFNAR1-deficient genetic background (Iversen et al., 2010; Iversen et al., 2015;
341 A. J. Lee et al., 2017; Leib et al., 1999; Reinert et al., 2012; Wang et al., 2012) and indicating an
342 early antiviral role (A. J. Lee et al., 2017; Luker, Prior, Song, Pica, & Leib, 2003). Rather, only
343 inhibition of sustained IFN signaling led to diminished disease with minimal impact on viral
344 control, thus revealing distinct antiviral and immunopathological effects of type I IFN signaling
345 that are temporally regulated and had heretofore been unappreciated during HSV-2 infection. The
346 source of sustained type I IFN production that promotes immunopathology after genital HSV-2
347 infection is currently unknown. HSV encodes numerous proteins that can suppress type I IFN
348 production and regulate the signaling pathways (Christensen et al., 2016; Lin & Zheng, 2019;
349 Melroe, DeLuca, & Knipe, 2004), suggesting that production of type I IFN likely occurs from a
350 cell type that is not directly infected. While plasmacytoid dendritic cells (pDC) are known as robust
351 producers of type I IFN, previous studies have demonstrated a limited role for pDCs in genital
352 HSV-2 infection (Swiecki, Wang, Gilfillan, & Colonna, 2013), indicating that there may be an
353 alternative source of type I IFN, such as conventional DCs (Wilson et al., 2013).

354 In humans, type I IFN can be detected at active lesion sites during recurrent episodes (Peng et al.,
355 2009; Roychoudhury et al., 2020), although levels do not correlate with restriction of viral
356 replication (Roychoudhury et al., 2020). This raises the possibility that type I IFN induction may
357 not be antiviral and could contribute to ulcer formation, although this hypothesis has yet to be
358 tested. Human neutrophils from females are also reported to be hyper-responsive to type I IFNs
359 (Gupta et al., 2020). Although clinical disease recurrence rates between men and women with
360 genital herpes are similar (Wald et al., 2002), differences in neutrophil sensitivity to type I IFN
361 may have implications for sex-dependent mechanisms of ulcer development.

362 Type I IFN signaling orchestrates a network of ISGs that limit viral infection using a wide
363 variety of mechanisms. In vitro stimulation of neutrophils with type I IFN leads to the upregulation
364 of many common ISGs as well as inflammatory genes, including IL-18 (Galani et al., 2017).
365 Importantly, it has been suggested that type I IFN can differentially regulate expression IL-18 and
366 IL-1 β , another IL-1 family cytokine that depends on caspase-mediated cleavage for activation
367 (Zhu & Kanneganti, 2017). It is currently unclear whether neutrophils are directly producing this
368 cytokine in our model of infection and whether IL-18 production is dependent on the classical
369 inflammasome-dependent route. As HSV also encodes proteins that can inhibit inflammasome
370 activity, including VP22 (Maruzuru et al., 2018), one possibility is that that the direct source of
371 IL-18 is a cell type that is not productively infected with HSV, such as neutrophils. Alternatively,
372 neutrophil proteases released in the extracellular space have been reported to cleave and activate
373 proIL-1 cytokines that are secreted by other cells in a caspase-1-independent manner (Clancy et
374 al., 2018; Robertson et al., 2006; Sugawara et al., 2001), suggesting a mechanism by which
375 neutrophils may modulate IL-18 levels without directly producing the cytokine themselves. Our
376 data show that along with neutrophils, IL-18 could be detected in the epithelium in cells that are

377 in close proximity to infiltrating neutrophils, indicating that there may be multiple sources and
378 mechanisms by which pathogenic IL-18 is produced during HSV-2 infection. Understanding these
379 mechanisms could further reveal novel, specific targets for therapeutics aimed at reducing
380 inflammation during genital herpes, and as such, are currently under investigation.

381 During HSV-2 vaginal infection, IL-18 stimulates NK cells to mediate rapid antiviral IFN γ
382 production upon infection (A. J. Lee et al., 2017), and previously thought to be important for
383 orchestrating a protective innate immune response. Accordingly, mice deficient in IL-18 are more
384 susceptible to HSV-2 infection (Harandi et al., 2001), as well as infection with HSV-1 through
385 multiple routes of inoculation (Fujioka et al., 1999; Reading et al., 2007), presumably due to
386 dysregulation of innate IFN γ production and loss of viral control. Our study reveals a novel aspect
387 of IL-18 biology during HSV-2 infection, and that like type I IFN signaling, there may be a
388 temporal component to the effects of IL-18 during HSV-2 infection. Therapeutic neutralization of
389 IL-18 did not alter viral titers in our model, suggesting that IL-18 does not have an impact on T
390 cell-dependent IFN γ production (Milligan & Bernstein, 1997; Nakanishi, Lu, Gerard, & Iwasaki,
391 2009) or direct antiviral activity. As previous studies have shown that IL-18 is also dispensable for
392 stimulating IFN γ from adaptive memory immune responses (Harandi et al., 2001), IL-18 may be
393 an attractive target for therapeutics aiming to reduce inflammation during genital herpes.
394 Currently, the mechanism by which IL-18 promotes disease during genital HSV-2 infection is
395 unknown. In the gut, the role of IL-18 is balanced between protection and pathology, depending
396 on the source of IL-18, the model of disease and the responsive cell type (Jarret et al., 2020;
397 Nowarski et al., 2015). The role of IL-18 during HSV-2 infection appears to be similarly complex,
398 and further study will be required to identify the compartment on which IL-18 acts and the
399 downstream effects of IL-18 signaling. Additionally, while our results demonstrate an important

400 role for IL-18, the reduction in disease severity is not as profound as when type I IFN signaling is
401 inhibited in our HSV-2 model of infection. Considering the complex response elicited by type I
402 IFN, our data allude to the possibility of other IL-18-independent, IFN-dependent mechanisms that
403 promote genital inflammation that have yet to be elucidated.

404 Synergistic effects of cytokine signaling have been reported to be important for
405 maximizing cellular responses to infection through the upregulation of cooperative or independent
406 molecular programs (Bartee & McFadden, 2013) or through the cross-regulation of receptor
407 signaling pathways (Ivashkiv & Donlin, 2014). Along with sustained type I IFN signaling during
408 HSV-2, the vaginal cytokine milieu also changes during the course of genital HSV-2 infection.
409 Whether the ISG profile induced in neutrophils by type I IFN signaling changes over the course
410 of acute HSV-2 infection, and whether this profile is affected by other cytokines, is unknown.
411 Upon activation, the activity of neutrophils responding to infection can be modulated strongly by
412 multiple interferons (IFNs), in a variety of tissues. Type I (Ank et al., 2008), type II (Iijima et al.,
413 2008; A. G. Lee et al., 2020) and type III IFNs (Ank et al., 2008; A. G. Lee et al., 2020) are all
414 robustly produced during HSV-2 infection. While type I and type II IFNs are crucial for control of
415 HSV-2 replication, endogenous type III IFNs do not appear to affect either disease severity or viral
416 control, although exogenous application of type III IFNs can reduce viral burden (Ank et al., 2008;
417 Ank et al., 2006). Expression of the type III IFN receptor, IFNLR, is limited to very few cell types,
418 including neutrophils and epithelial cells (Blazek et al., 2015; Mahlaköiv, Hernandez, Gronke,
419 Diefenbach, & Staeheli, 2015; Sommereyns, Paul, Staeheli, & Michiels, 2008). As epithelial cells
420 are a major target for HSV-2 replication, dissecting the action of type III IFNs within the neutrophil
421 and epithelial cell compartments may reveal a more detailed picture of the role type III IFNs play.
422 The impact of simultaneous type I, II and III IFN signaling on neutrophil function is currently

423 unclear and due to the importance of these molecules, as well as PRRs, in controlling infection,
424 cell-specific modifications of receptor expression will be required for further investigation.

425 Beyond their inflammatory role during HSV-2 infection, this study and others (S. Li et al.,
426 2018; Milligan, 1999) have demonstrated that neutrophils can be found in the vagina at steady
427 state. Detection of neutrophils in washes collected from the vaginal lumen suggest that the
428 neutrophils are actively extravasating, migrating through the lamina propria and through the
429 epithelial barrier. Previous studies have indicated that in mice, recruitment of neutrophils into the
430 vagina is regulated by hormone-dependent expression of chemokines, including CXCR2 ligands,
431 in the tissue (Lasarte et al., 2016). In humans, the number of neutrophils in the fluctuates with the
432 hormone cycle in the upper reproductive tract, but reportedly remains stable in the lower tract
433 (Wira, Rodriguez-Garcia, & Patel, 2015). It is unclear why neutrophils actively patrol the vagina
434 even in the absence of infection, what consequences their immunosurveillance has on the normal
435 physiology of the reproductive tract, and how the tissue microenvironment affects the biology of
436 the neutrophils themselves. In the oral mucosa, constant recruitment of neutrophils into the tissue
437 helps support the maintenance of a healthy microbiome (Uriarte, Edmisson, & Jimenez-Flores,
438 2016), while molecular products derived from the microbiome such as peptidoglycan can support
439 basal activity of neutrophils (Clarke et al., 2010). Whether similar interactions between the vaginal
440 neutrophils and the vaginal microbiome also occur is unknown. Furthermore, due to the lack of
441 tractable animal models, the role of neutrophils in other common non-viral STIs is unclear,
442 although neutrophils appear to play a similar pathological role in the upper reproductive tract after
443 Chlamydia infection (Lijek, Helble, Olive, Seiger, & Starnbach, 2018). In summary, our study
444 reveals that pathology during genital HSV-2 infection is driven at least in part by a robust

445 neutrophil response, and lays the foundation for identifying the host pathways that may be targeted

446 to help ameliorate disease.

447

448 **ACKNOWLEDGEMENTS**

449 We thank Rachel Idol, Antonina Akk and Celeste Cummings for technical assistance on assays
450 used in this study. This work was supported by grants from the NIH (HS: R01 AI134962) and
451 Children's Discovery Institute (RAC). T.J.L was supported by funding for the Training Program
452 in Immunology from the NIH (T32 AI007163).

453

454 **Author contributions**

455 T.J.L, Y.S.L., A.C., M.R.F., J.M.S., A.N.O., X.J., and H.S. designed and conducted experiments,
456 acquired data and analyzed data. R.A.C., C.T.N.P, and M.C.D. aided in the design of experiments.
457 P.S.A. and M.A. analyzed data. H.S. and Y.S.L. wrote the manuscript, and all authors edited the
458 final version of the paper.

459

460 **Declaration of Interests**

461 The authors declare no competing interests.

462 **FIGURE SUPPLEMENTS**

463 Figure 1 - Supplement 1. Neutrophil depletion does not affect magnitude of the immune cell
464 response after HSV-2 infection.

465 Figure 1 - Supplement 2. PAD4 is not required for development of genital inflammation during
466 HSV-2 infection.

467 Figure 1 - Supplement 3. ROS production and STIM1/STIM2 expression in neutrophils are not
468 required for genital inflammation after HSV-2 infection

469 Figure 2 - Supplement 1. Neutrophil depletion prior to HSV-1 genital infection has little impact
470 on disease progression.

471 Figure 3 - Supplement 1. Validation of ISG expression in the vagina.

472 Figure 3 - Supplement 3. Type I IFN is robustly produced in the vagina early after acute HSV-1
473 or HSV-2 infection.

474 Figure 4 - Supplement 1. Early blockade of IFNAR1 leads to accelerated and more severe disease
475 after HSV-2 infection.

476 Figure 6 - Supplement 1. Neutrophils do not control production of common pro-inflammatory and
477 antiviral cytokines during HSV-2 infection.

478

479 **SOURCE DATA**

480 Source data files have been provided for all figures and figure supplements.

481

482 **METHODS**

483 **Mice.** Six-week old female C57BL/6J mice were purchased from Jackson Laboratories and
484 rested for at least one week and infected at a minimum of seven weeks of age. Ncf2 KO mice and
485 controls were provided by M.C. Dinauer (Washington University, St Louis) and generated as
486 previously described (Jacob et al., 2017). Stim1^{fl/fl} x Stim2^{fl/fl} x MRP8-Cre mice were provided by
487 G.A. Clemens (Washington University, St Louis) and were generated as previously described
488 (Clemens et al., 2017). IFNAR1^{fl/fl} mice (Ifnar1^{tm1Uka}) were a gift from H.W. Virgin (Kamphuis,
489 Junt, Waibler, Forster, & Kalinke, 2006; Nice et al., 2016). PAD4^{fl/fl} mice (B6(Cg)-
490 Padi4^{tm1.2Kmw/J}) and MRP8-Cre (B6.Cg-Tg(S100A8-cre,-EGFP)1Ilw/J) were obtained from
491 Jackson Laboratories and bred at Washington University School of Medicine. Cre- littermates
492 generated from breeding pairs were used as controls. All mice were maintained on a 12 hour
493 light/dark cycle with unlimited access to food and water. This study was carried out in accordance
494 with the recommendations in the Guide for the Care and Use of Laboratory Animals of the National
495 Institutes of Health.

496 **Ethics statement.** The protocols were approved by the Institutional Animal Care and use
497 Committee (IACUC) at the Washington University School of Medicine (Assurance number
498 A3381-01). All experiments were performed under biosafety level 2 (A-BSL2) containment and
499 all efforts were made to minimize animal suffering.

500 **Cell lines and primary cells.** Vero Cells (African green monkey kidney epithelial cells,
501 ATCC) were cultured in Dulbecco's Modified Eagle Medium (Gibco) containing 1% fetal bovine
502 serum (FBS, Corning) and maintained at 37°C with 5% CO₂. Primary neutrophils were isolated
503 from the bone marrow (BM) of naive female C57BL/6J mice. A Histopaque gradient was used to
504 isolate primary neutrophils for Reactive Oxygen Species (ROS) assays, while a Percoll gradient

505 was used for NET assays. For Histopaque isolation: 3ml of Histopaque 1119 (Sigma-Aldrich) was
506 overlaid with 3ml of Histopaque 1077 (Sigma-Aldrich). A single cell suspension of isolated BM
507 cells in 1ml of PBS was layered over the Histopaque gradient. Cells were centrifuged for 30
508 minutes at room temperature (RT), and neutrophils were collected from the bottom interface. For
509 Percoll isolation: BM cells were resuspended in HBSS (Gibco) with 20mM HEPES (Gibco) and
510 layered over 6ml of 62% Percoll solution (GE Healthcare). Cells were centrifuged for 30 minutes
511 at RT, and neutrophils were collected from the bottom of the tube. All tissue culture experiments
512 were performed under BSL2 containment.

513 ***Viruses and virus quantification.*** WT HSV-2 186 syn+ (Spang, Godowski, & Knipe,
514 1983) and HSV-1 McKrae (Williams, Nesburn, & Kaufman, 1965) was propagated and titered on
515 Vero cells as previously described (A. G. Lee et al., 2020). Briefly, for propagation of virus stocks,
516 Vero cells were plated in T150 tissue culture flasks, inoculated at 0.01 MOI at 80% confluence
517 and incubated at 37°C. Infected cells were harvested 2-3 days after infection, resuspended in equal
518 volumes of virus supernatant and twice-autoclaved milk, and sonicated. Lysed cells were aliquoted
519 and used as viral stock. To titer, Vero cells were plated in 6-well plates and inoculated with 10-
520 fold serial dilutions of stock virus. After inoculation, overlay media with 20µg/ml human IgG was
521 added to each well and plates were incubated at 37°C for 2-3 days. To count, Vero cells were
522 stained with 0.1% crystal violet. All tissue culture experiments were performed under BSL2
523 containment. For titration of virus in the vaginal lumen, 50ul washes with sterile PBS were
524 collected using a pipette and a sterile calginate swab, and diluted in 950ul of ABC buffer (0.5mM
525 CaCl₂, 0.5mM MgCl₂, 1% glucose, 1% fetal bovine serum (FBS) in sterile PBS). 10-fold serial
526 dilution of vaginal washes were titered by plaque assays won Vero cells (A. G. Lee et al., 2020).

527 ***Mouse infection studies.*** All mice were injected subcutaneously in the neck ruff once
528 with 2mg of DMPA (Depo-Provera, Pfizer) 5-7 days prior to virus inoculation. For experiments
529 in which neutrophils were depleted, mice were intraperitoneally (i.p.) injected once with 500µg of
530 anti-Ly6G (clone 1A8) or rat IgG2a isotype control (anti-trinitrophenol+KLH) (Leinco
531 Technologies) diluted in sterile phosphate buffered saline (PBS, Sigma-Aldrich) 1 day prior to
532 inoculation. For experiments in which IFNAR blockade was conducted, mice were i.p. injected
533 once with 1mg of anti-IFNAR1 (clone MAR1-5A3) or mouse IgG1 isotype control (clone HKSP)
534 (Leinco Technologies) on either the day of inoculation ("early") or at 4 d.p.i. ("late"). For "late"
535 treatments, only mice without overt signs of genital inflammation were chosen for antibody
536 injection in both anti-IFNAR and isotype control groups to avoid biasing of results. For
537 experiments in which IL-18 was neutralized, mice were treated intravaginally with 100µg of anti-
538 IL-18 antibody (clone YIGIF74-1G7) or rat IgG2a isotype control (clone 2A3) (BioXCell) on days
539 3-5 after infection. Selection of mice for isotype control or experimental antibody treatment was
540 random. For intravaginal inoculation, a sterile calginate swab (McKesson) moistened with sterile
541 PBS was used to gently disrupt mucous from the vaginal cavity. Stock virus was diluted in sterile
542 PBS and either 5000 PFU or 10⁴ PFU virus was delivered into the vaginal cavity via pipette tip in
543 a 10µl volume. Mice were weighed and monitored for signs of disease for 1 week following
544 infection and monitored for survival for 2 weeks. Genital inflammation was scored as follows: 0 -
545 no inflammation, 1 - mild redness and swelling around the vaginal opening, 2 - fur loss and visible
546 ulceration, 3 - severe ulceration and mild signs of sickness behavior (lack of grooming), 4 -
547 hindlimb paralysis, and 5 - moribund.

548 ***Vaginal tissue processing.*** All tissues were harvested from animals sedated with ketamine
549 and xylazine and thoroughly perfused with a minimum of 15ml of PBS. Vaginas were processed

550 as follows: tissue was cut into pieces and digested for 15 minutes in a shaking water bath held at
551 37°C in a 0.5mg/ml solution of Dispase II (Roche) in PBS. Tissues were then transferred to a
552 solution of 0.5mg/ml Collagenase D (Roche) and 15µg/ml DNase I (Roche) in RPMI media
553 (Gibco) supplemented with 10% fetal bovine serum (FBS, Corning) and 1% pen/strep (Gibco) and
554 digested for 25 minutes in a shaking water bath held at 37°C. 50µl of sterile EDTA was added to
555 each sample and incubated at 37°C for another 5 minutes. Tissue were then mechanically disrupted
556 through a 70-um cell strainer into a single cell suspension using a 3ml syringe plunger. Tissues
557 were washed with RPMI media with 1% FBS, centrifuged, and resuspended in 200µl RPRM with
558 1% FBS and 1% pen/strep.

559 **Flow cytometry.** Single cell suspensions from vaginal tissues, or luminal cells collected in
560 vaginal washes were plated in 96-well plates and incubated with Live/Dead Fixable Aqua Dead
561 Cell Stain kit (Molecular Probes) for 15 minutes at room temperature (RT) in the dark. Cells were
562 then incubated with Fc block (anti-CD16/32, Biolegend) for 15 minutes at RT in the dark. Surface
563 staining was performed in FACS buffer (1% FBS and 0.02% sodium azide in PBS) on ice and in
564 the dark using the following antibodies: CD3 (clone 145-2C11), CD4 (clone GK1.5), CD8a (clone
565 53-6.7), CD11b (clone M1/70), CD45 (clone 30-F11), Gr-1 (clone RB6-8C5), Ly6C (clone
566 HK1.4), Ly6G (clone 1A8), and NK1.1 (clone PK136). All antibodies were purchased from
567 Biolegend. For surface staining of IFNAR1, cells were incubated with an anti-IFNAR1 antibody
568 or a mouse IgG1 isotype control (Leinco Technologies) for 20 minutes at 37°C. Cells were washed
569 and then surface staining of other markers proceeded as described above. Cell counts were
570 performed by adding Precision Count Beads (Biolegend) to samples prior to flow cytometric
571 acquisition. Samples were acquired on an LSR Fortessa (BD Biosciences) and analyzed by FlowJo
572 (Treestar).

573 ***Tissue immunofluorescent (IF) staining and immunohistochemistry (IHC).*** All tissues
574 were harvested from animals sedated with ketamine and xylazine and thoroughly perfused with a
575 minimum of 15ml of PBS, followed by 15ml of PLP fixative (0.01M NaIO₄, 0.075M lysine,
576 0.0375M sodium phosphate, 2% paraformaldehyde (PFA)) for IF or 4% PFA for IHC. Tissues
577 were cryoprotected in 30% sucrose, frozen in OCT medium (Sakura) and cut into 7µm sections.
578 Cryosections were blocked 5% bovine serum albumin (BSA), 5% goat serum (Jackson
579 Immunoresearch) and 0.1% Triton-X in PBS for 1 hour at RT. HSV antigens were detected with
580 a rabbit anti-HSV primary antibody (Dako), incubated overnight at 4°C, washed in PBS and
581 incubated for 1 hour at RT with a goat anti-rabbit IgG conjugated to AlexaFluor 488 (Life
582 Technologies). S100A8 was detected with a rat anti-mouse S100A8 primary antibody (clone
583 63N13G5, Novus Biologicals) and a goat anti-rat IgG conjugated to AlexaFluor 568 (Life
584 Technologies) in a similar manner. IL-18 was detected using a biotinylated rat anti-mouse IL-18
585 primary antibody (clone 93-10C, MBL International). Cryosections were blocked as described
586 above, and then treated with the Avidin/Biotin Blocking Kit (Vector Laboratories) according to
587 manufacturer's protocol. Endogenous peroxidases were quenched with a 2 % hydrogen peroxide
588 solution. Anti-mouse IL-18 or a rat IgG1 isotype control were incubated overnight at 4°C. The
589 AlexaFluor 647 Tyramide Signal Amplification kit (Invitrogen) was used to visualize IL-18 and
590 used according to manufacturer's protocol. DNA was visualized with 4',6-diamidino-2-
591 phenylindole (DAPI) (Life Technologies). Sections were imaged with a Zeiss Cell Observer
592 inverted microscope using a 40x objective, acquired with Zen software and image brightness was
593 adjusted using Photoshop (Adobe). For IHC, sections were probed with an anti-HSV antibody
594 incubated overnight at 4°C (Dako), a donkey anti-rabbit IgG-HRP antibody (Jackson
595 Immunoresearch) for 1 hr at RT and then enzymatically visualized by 3,3'-diaminobenzidine

596 (DAB) enzyme reaction (Sigma-Aldrich). Sections were counterstained with hematoxylin and
597 eosin and images were captured using Zeiss ZEN software on a Zeiss Cell Observer inverted
598 microscope with an AxioCam dual B/W and color camera with a 20x objective. Image brightness
599 was adjusted using Photoshop (Adobe) and merged with Image J64 (NIH).

600 ***RNA extraction and quantitative reverse transcription (RT)-PCR.*** Harvested tissues were
601 homogenized in RLT buffer (RNeasy Kit, Qiagen) with approximately 100 μ l of sterile 1.0mm
602 zirconia/silica beads (Biospec Products) in a bead beater. Homogenized tissue samples were
603 processed according to manufacturer's protocol using the RNeasy Mini Kit (Qiagen) and RNA
604 quality and quantity was assessed on a Nanodrop (ThermoFisher). qRT-PCR was performed in
605 10 μ l reactions using the iTaq Universal SYBR Green One-Step kit (Biorad) according to
606 manufacturer's protocol.

607 ***Single cell RNA-sequencing preparation.*** Single cell suspensions from digested vaginas
608 were stained with Live/Dead Fixable Aqua Dead Cell Stain kit (Molecular Probes) for 15 minutes
609 at room temperature (RT) in the dark. Live cells were sorted on BD FACS Aria II housed in a BSL2
610 biosafety cabinet. A minimum of 16,000 cells were resuspended in PBS with 2% FBS and 0.2U/ μ l
611 RNase inhibitor at a concentration of 800-1400 cells/ μ l, submitted to McDonnell Genome Institute
612 and prepared for droplet-based 3' end single-cell RNA sequencing using the Chromium 3' v3 single
613 cell reagent kit per manufacturer's protocol (10x Genomics). Library sequencing was performed
614 on a NovaSeq S4 (Illumina).

615 ***Cytokine measurement.*** For cytokine analysis by Bio-Plex Pro Mouse Cytokine 23-Plex
616 Immunoassay (Bio-rad): 2 x 50 μ l washes with sterile PBS were collected from the vaginal lumen
617 using a pipette. Samples were centrifuged for 3 minutes at 13000*g to remove mucous and cells,
618 and supernatants were added to 200 μ l of ABC buffer. The assay was performed according to

619 manufacturer instructions, and plates were read on a Luminex Bioplex 100 system (Biorad). For
620 measurement of IL-18, 2 x 50 μ l washes with sterile PBS were collected from the vaginal lumen
621 and centrifuged to remove mucous and cells. IL-18 was measured using the mouse IL-18 ELISA
622 kit (MBL International) according to manufacturer's instructions at half-volumes.

623 ***In vitro neutrophil stimulation.*** To measure ROS production, isolated neutrophils were
624 stimulated with heat-killed HSV-2 (56°C for 30 minutes) at an MOI of 5 for 16 hours at 37°C.
625 ROS levels were quantified using DCFDA Cellular ROS Detection Assay kit (Abcam) according
626 to manufacturer protocol. Fluorescence levels were measured by flow cytometry. To induce NET
627 formation, neutrophils were stimulated with heat-killed HSV-2 at an MOI of 1 for 4 hours at 37°C.
628 Cells were fixed with 8% PFA overnight and probed with a polyclonal rabbit antibody against
629 mouse citrullinated histone H3 (Abcam) for 1 hour at RT in 1% BSA and 0.1% Triton-X for 1
630 hour at RT, a goat anti-rabbit antibody conjugated to AlexaFluor 488 (Life Technologies) for 1
631 hour at RT and DAPI diluted in PBS for 6 minutes at RT. Cells were imaged with a Zeiss Cell
632 Observer inverted microscope using a 63x objective and image brightness was adjusted using
633 Photoshop (Adobe).

634 ***Single cell RNA-sequencing analysis.***

635 ***Processing data with Seurat package:*** The Seurat package in R was used for analysis
636 (Butler, Hoffman, Smibert, Papalexi, & Satija, 2018). Cells with mitochondrial content greater
637 than 5% were removed. The initial analysis of the data revealed three clusters of the cells that had
638 extremely low levels of detected genes (i.e. <500) which were then filtered out as non-viable cells.
639 Remaining cells were used for downstream analysis, resulting in the 6,507 cells per sample that
640 passed quality control (QC) and filtering. Filtered data were normalized using a scaling factor of
641 10,000, and nUMI was regressed with a negative binomial model.

642 *Normalization and Feature Selection:* After the data filtration, data were normalized using
643 a scaling factor of 10,000 and log transformed. The highly variable genes were selected using the
644 FindVariableFeatures function with mean greater than 0.0125 or less than 3 and dispersion greater
645 than 0.5. These genes were used in performing the linear dimensionality reduction.

646 *Clustering and Finding Markers:* Principal component analysis was performed using the
647 top 3000 most variable genes prior to clustering and number of the first principal components
648 (PCs) were used based on the ElbowPlot as described below for different datasets. Clustering was
649 performed using the FindClusters function which works on K-nearest neighbor (KNN) graph
650 model with the granularity (resolution) ranging from 0.1-1.5. The datasets were projected as t-SNE
651 plots.

652 ***Statistical analysis.*** All numerical data analysis except for scRNA-seq data analysis was
653 performed on Graphpad Prism8 software. Values were log-transformed to normalize distribution
654 and variances where necessary. Immune cell numbers and cytokine measurement were analyzed
655 by 2-way ANOVA with Bonferroni multiple comparisons test. Log-transformed viral titers were
656 analyzed by repeated measures two-way ANOVA with Bonferroni multiple comparisons test.
657 Inflammation scores were analyzed by repeated-measures two-way ANOVA or mixed-effects
658 analysis with Geisser-Greenhouse correction and Bonferroni's multiple comparisons test. The
659 Geisser-Greenhouse correction was used for inflammation scores to correct any violations of
660 sphericity and to provide a more restrictive, stringent calculation of p values. ROS MFI was
661 measured by unpaired two-tailed Student's t-test. qPCR results were analyzed by one-way
662 ANOVA with Tukey's multiple comparisons test. A $p < 0.05$ was considered statistically
663 significant. No experimental data points were excluded from statistical analysis, including
664 potential outliers. Mouse and sample numbers per group and experimental repeat information is

665 provided in the figure legends. All data points represent individual biological replicates, and the
666 'n' for each group refers to biological replicates. No power calculations were performed to
667 determine sample size; rather sample sizes were determined based on historical data.

668 **DATA AVAILABILITY**

669 The published article includes partial data from a single cell RNA-sequencing dataset generated
670 during this study. These data are available at Gene Expression Omnibus (GEO) (accession code
671 GSE161336). The key to access this data is sngheymjxqbjns.

672

673 **REFERENCES**

- 674 Akk, A., Springer, L. E., & Pham, C. T. N. (2016). Neutrophil Extracellular Traps Enhance Early
675 Inflammatory Response in Sendai Virus-Induced Asthma Phenotype. *Frontiers in*
676 *Immunology*, 7, 325. doi:10.3389/fimmu.2016.00325
- 677 Ank, N., Iversen, M. B., Bartholdy, C., Staeheli, P., Hartmann, R., Jensen, U. B., . . . Paludan, S.
678 R. (2008). An Important Role for Type III Interferon (IFN- λ /IL-28) in TLR-Induced
679 Antiviral Activity. *The Journal of Immunology*, 180(4), 2474.
680 doi:10.4049/jimmunol.180.4.2474
- 681 Ank, N., West, H., Bartholdy, C., Eriksson, K., Thomsen, A. R., & Paludan, S. R. (2006). Lambda
682 interferon (IFN-lambda), a type III IFN, is induced by viruses and IFNs and displays potent
683 antiviral activity against select virus infections in vivo. *Journal of Virology*, 80(9), 4501-
684 4509. doi:10.1128/JVI.80.9.4501-4509.2006
- 685 Bai, F., Kong, K.-F., Dai, J., Qian, F., Zhang, L., Brown, C. R., . . . Montgomery, R. R. (2010). A
686 paradoxical role for neutrophils in the pathogenesis of West Nile virus. *The Journal of*
687 *Infectious Diseases*, 202(12), 1804-1812. doi:10.1086/657416
- 688 Bartee, E., & McFadden, G. (2013). Cytokine synergy: An underappreciated contributor to innate
689 anti-viral immunity. *Cytokine*, 63(3), 237-240.
690 doi:<https://doi.org/10.1016/j.cyto.2013.04.036>
- 691 Blazek, K., Eames, H. L., Weiss, M., Byrne, A. J., Perocheau, D., Pease, J. E., . . . Udalova, I. A.
692 (2015). IFN- λ resolves inflammation via suppression of neutrophil infiltration and IL-1 β
693 production. *The Journal of Experimental Medicine*, 212(6), 845-853.
694 doi:10.1084/jem.20140995

- 695 Boddington, J., Dijkman, H., Hendriksen, E., Schiff, R., & Stolz, E. (1987). HSV-2 replication
696 sites, monocyte and lymphocytic cell infection and virion phagocytosis by neutrophils, in
697 vesicular lesions on penile skin. *Journal of Cutaneous Pathology*, *14*(3), 165-175.
698 doi:10.1111/j.1600-0560.1987.tb00492.x
- 699 Brandes, M., Klauschen, F., Kuchen, S., & Germain, R. N. (2013). A systems analysis identifies a
700 feedforward inflammatory circuit leading to lethal influenza infection. *Cell*, *154*(1), 197-
701 212. doi:10.1016/j.cell.2013.06.013
- 702 Butler, A., Hoffman, P., Smibert, P., Papalexi, E., & Satija, R. (2018). Integrating single-cell
703 transcriptomic data across different conditions, technologies, and species. *Nature*
704 *Biotechnology*, *36*(5), 411-420. doi:10.1038/nbt.4096
- 705 Cheng, L., Yu, H., Li, G., Li, F., Ma, J., Li, J., . . . Su, L. (2017). Type I interferons suppress viral
706 replication but contribute to T cell depletion and dysfunction during chronic HIV-1
707 infection. *JCI Insight*, *2*(12). doi:10.1172/jci.insight.94366
- 708 Christensen, M. H., Jensen, S. B., Miettinen, J. J., Luecke, S., Prabakaran, T., Reinert, L. S., . . .
709 Paludan, S. R. (2016). HSV-1 ICP27 targets the TBK1-activated STING signaling to
710 inhibit virus-induced type I IFN expression. *The EMBO journal*, *35*(13), 1385-1399.
711 doi:10.15252/emboj.201593458
- 712 Clancy, D. M., Sullivan, G. P., Moran, H. B. T., Henry, C. M., Reeves, E. P., McElvaney, N. G., .
713 . . Martin, S. J. (2018). Extracellular Neutrophil Proteases Are Efficient Regulators of IL-
714 1, IL-33, and IL-36 Cytokine Activity but Poor Effectors of Microbial Killing. *Cell*
715 *Reports*, *22*(11), 2937-2950. doi:<https://doi.org/10.1016/j.celrep.2018.02.062>
- 716 Clarke, T. B., Davis, K. M., Lysenko, E. S., Zhou, A. Y., Yu, Y., & Weiser, J. N. (2010).
717 Recognition of peptidoglycan from the microbiota by Nod1 enhances systemic innate

- 718 immunity. *Nat Med*, 16(2), 228-231.
719 doi:http://www.nature.com/nm/journal/v16/n2/supinfo/nm.2087_S1.html
- 720 Clemens, R. A., Chong, J., Grimes, D., Hu, Y., & Lowell, C. A. (2017). STIM1 and STIM2
721 cooperatively regulate mouse neutrophil store-operated calcium entry and cytokine
722 production. *Blood*, 130(13), 1565. Retrieved from
723 <http://www.bloodjournal.org/content/130/13/1565.abstract>
- 724 Dinauer, M. C. (2019). Inflammatory consequences of inherited disorders affecting neutrophil
725 function. *Blood*, 133(20), 2130-2139. doi:10.1182/blood-2018-11-844563
- 726 Divito, S. J., & Hendricks, R. L. (2008). Activated inflammatory infiltrate in HSV-1-infected
727 corneas without herpes stromal keratitis. *Investigative ophthalmology & visual science*,
728 49(4), 1488-1495. doi:10.1167/iovs.07-1107
- 729 Fujioka, N., Akazawa, R., Ohashi, K., Fujii, M., Ikeda, M., & Kurimoto, M. (1999). Interleukin-
730 18 Protects Mice against Acute Herpes Simplex Virus Type 1 Infection. *Journal of*
731 *Virology*, 73(3), 2401-2409. Retrieved from <http://jvi.asm.org/content/73/3/2401.abstract>
- 732 Galani, I. E., & Andreakos, E. (2015). Neutrophils in viral infections: Current concepts and
733 caveats. *Journal of Leukocyte Biology*, 98(4), 557-564. doi:10.1189/jlb.4VMR1114-555R
- 734 Galani, I. E., Triantafyllia, V., Eleminiadou, E.-E., Koltsida, O., Stavropoulos, A., Manioudaki,
735 M., . . . Andreakos, E. (2017). Interferon- λ Mediates Non-redundant Front-Line Antiviral
736 Protection against Influenza Virus Infection without Compromising Host Fitness.
737 *Immunity*, 46(5), 875-890.e876. doi:<https://doi.org/10.1016/j.immuni.2017.04.025>
- 738 Gill, N., Deacon, P. M., Lichty, B., Mossman, K. L., & Ashkar, A. A. (2006). Induction of Innate
739 Immunity against Herpes Simplex Virus Type 2 Infection via Local Delivery of Toll-Like

- 740 Receptor Ligands Correlates with Beta Interferon Production. *Journal of Virology*, 80(20),
741 9943-9950. doi:10.1128/jvi.01036-06
- 742 Gopinath, S., Kim, M. V., Rakib, T., Wong, P. W., van Zandt, M., Barry, N. A., . . . Iwasaki, A.
743 (2018). Topical application of aminoglycoside antibiotics enhances host resistance to viral
744 infections in a microbiota-independent manner. *Nature Microbiology*, 3(5), 611-621.
745 doi:10.1038/s41564-018-0138-2
- 746 Gosmann, C., Anahtar, M. N., Handley, S. A., Farcasanu, M., Abu-Ali, G., Bowman, B. A., . . .
747 Kwon, D. S. (2017). Lactobacillus-Deficient Cervicovaginal Bacterial Communities Are
748 Associated with Increased HIV Acquisition in Young South African Women. *Immunity*,
749 46(1), 29-37. doi:<http://dx.doi.org/10.1016/j.immuni.2016.12.013>
- 750 Granger, V., Peyneau, M., Chollet-Martin, S., & de Chaisemartin, L. (2019). Neutrophil
751 Extracellular Traps in Autoimmunity and Allergy: Immune Complexes at Work. *Frontiers*
752 *in Immunology*, 10(2824). doi:10.3389/fimmu.2019.02824
- 753 Gupta, S., Nakabo, S., Blanco, L. P., O'Neil, L. J., Wigerblad, G., Goel, R. R., . . . Kaplan, M. J.
754 (2020). Sex differences in neutrophil biology modulate response to type I interferons and
755 immunometabolism. *Proceedings of the National Academy of Sciences*, 117(28), 16481-
756 16491. doi:10.1073/pnas.2003603117
- 757 Harandi, A. M., Svennerholm, B., Holmgren, J., & Eriksson, K. (2001). Interleukin-12 (IL-12) and
758 IL-18 are important in innate defense against genital herpes simplex virus type 2 infection
759 in mice but are not required for the development of acquired gamma interferon-mediated
760 protective immunity. *Journal of Virology*, 75(14), 6705-6709.
761 doi:10.1128/JVI.75.14.6705-6709.2001

- 762 Harris, L. D., Tabb, B., Sodora, D. L., Paiardini, M., Klatt, N. R., Douek, D. C., . . . Estes, J. D.
763 (2010). Downregulation of Robust Acute Type I Interferon Responses Distinguishes
764 Nonpathogenic Simian Immunodeficiency Virus (SIV) Infection of Natural Hosts from
765 Pathogenic SIV Infection of Rhesus Macaques. *Journal of Virology*, *84*(15), 7886-7891.
766 doi:10.1128/jvi.02612-09
- 767 Horbul, J. E., Schmechel, S. C., Miller, B. R. L., Rice, S. A., & Southern, P. J. (2011). Herpes
768 Simplex Virus-Induced Epithelial Damage and Susceptibility to Human
769 Immunodeficiency Virus Type 1 Infection in Human Cervical Organ Culture. *PLoS ONE*,
770 *6*(7), e22638. doi:10.1371/journal.pone.0022638
- 771 Iijima, N., Linehan, M. M., Zamora, M., Butkus, D., Dunn, R., Kehry, M. R., . . . Iwasaki, A.
772 (2008). Dendritic cells and B cells maximize mucosal Th1 memory response to herpes
773 simplex virus. *The Journal of Experimental Medicine*, *205*(13), 3041-3052.
774 doi:10.1084/jem.20082039
- 775 Iijima, N., Mattei, L. M., & Iwasaki, A. (2011). Recruited inflammatory monocytes stimulate
776 antiviral Th1 immunity in infected tissue. *Proceedings of the National Academy of Sciences*
777 *of the United States of America*, *108*(1), 284-289. doi:10.1073/pnas.1005201108
- 778 Ivashkiv, L. B., & Donlin, L. T. (2014). Regulation of type I interferon responses. *Nature reviews*.
779 *Immunology*, *14*(1), 36-49. doi:10.1038/nri3581
- 780 Iversen, M. B., Ank, N., Melchjorsen, J., & Paludan, S. R. (2010). Expression of type III interferon
781 (IFN) in the vaginal mucosa is mediated primarily by dendritic cells and displays stronger
782 dependence on NF-kappaB than type I IFNs. *Journal of Virology*, *84*(9), 4579-4586.
783 doi:10.1128/JVI.02591-09

- 784 Iversen, M. B., Reinert, L. S., Thomsen, M. K., Bagdonaite, I., Nandakumar, R., Cheshenko, N., .
785 . . Paludan, S. R. (2015). An innate antiviral pathway acting before interferons at epithelial
786 surfaces. *Nat Immunol, advance online publication*. doi:10.1038/ni.3319
787 <http://www.nature.com/ni/journal/vaop/ncurrent/abs/ni.3319.html#supplementary-information>
- 788 Iversen, M. B., Reinert, L. S., Thomsen, M. K., Bagdonaite, I., Nandakumar, R., Cheshenko, N., .
789 . . Paludan, S. R. (2016). An innate antiviral pathway acting before interferons at epithelial
790 surfaces. *Nature immunology*, 17(2), 150-158. doi:10.1038/ni.3319
- 791 Jacob, C. O., Yu, N., Yoo, D.-G., Perez-Zapata, L. J., Barbu, E. A., Kaplan, M. J., . . . Dinauer, M.
792 C. (2017). Haploinsufficiency of NADPH Oxidase Subunit Neutrophil Cytosolic Factor 2
793 Is Sufficient to Accelerate Full-Blown Lupus in NZM 2328 Mice. *Arthritis &*
794 *Rheumatology*, 69(8), 1647-1660. doi:10.1002/art.40141
- 795 Jacquelin, B., Mayau, V., Targat, B., Liovat, A.-S., Kunkel, D., Petitjean, G., . . . Müller-Trutwin,
796 M. C. (2009). Nonpathogenic SIV infection of African green monkeys induces a strong but
797 rapidly controlled type I IFN response. *The Journal of Clinical Investigation*, 119(12),
798 3544-3555. doi:10.1172/JCI40093
- 799 Jarret, A., Jackson, R., Duizer, C., Healy, M. E., Zhao, J., Rone, J. M., . . . Flavell, R. A. (2020).
800 Enteric Nervous System-Derived IL-18 Orchestrates Mucosal Barrier Immunity. *Cell*,
801 180(1), 50-63.e12. doi:<https://doi.org/10.1016/j.cell.2019.12.016>
- 802 Jenne, C. N., & Kubes, P. (2015). Virus-induced NETs--critical component of host defense or
803 pathogenic mediator? *PLOS Pathogens*, 11(1), e1004546-e1004546.
804 doi:10.1371/journal.ppat.1004546
- 805 Jenne, Craig N., Wong, Connie H. Y., Zemp, Franz J., McDonald, B., Rahman, Masmudur M.,
806 Forsyth, Peter A., . . . Kubes, P. (2013). Neutrophils Recruited to Sites of Infection Protect

- 807 from Virus Challenge by Releasing Neutrophil Extracellular Traps. *Cell Host & Microbe*,
808 *13*(2), 169-180. doi:<http://dx.doi.org/10.1016/j.chom.2013.01.005>
- 809 Kamphuis, E., Junt, T., Waibler, Z., Forster, R., & Kalinke, U. (2006). Type I interferons directly
810 regulate lymphocyte recirculation and cause transient blood lymphopenia. *Blood*, *108*(10),
811 3253-3261. doi:10.1182/blood-2006-06-027599
- 812 Kaushic, C., Ashkar, A. A., Reid, L. A., & Rosenthal, K. L. (2003). Progesterone Increases
813 Susceptibility and Decreases Immune Responses to Genital Herpes Infection. *The Journal*
814 *of Virology*, *77*(8), 4558-4565. Retrieved from
815 <http://jvi.asm.org/cgi/content/abstract/77/8/4558>
- 816 Khoury-Hanold, W., Yordy, B., Kong, P., Kong, Y., Ge, W., Szigeti-Buck, K., . . . Iwasaki, A.
817 (2016). Viral Spread to Enteric Neurons Links Genital HSV-1 Infection to Toxic
818 Megacolon and Lethality. *Cell Host & Microbe*, *19*(6), 788-799.
819 doi:<http://dx.doi.org/10.1016/j.chom.2016.05.008>
- 820 Krzyzowska, M., Baska, P., Grochowska, A., Orłowski, P., Nowak, Z., & Winnicka, A. (2014).
821 Fas/FasL pathway participates in resolution of mucosal inflammatory response early
822 during HSV-2 infection. *Immunobiology*, *219*(1), 64-77.
823 doi:<http://dx.doi.org/10.1016/j.imbio.2013.08.002>
- 824 Kulkarni, U., Zemans, R. L., Smith, C. A., Wood, S. C., Deng, J. C., & Goldstein, D. R. (2019).
825 Excessive neutrophil levels in the lung underlie the age-associated increase in influenza
826 mortality. *Mucosal immunology*, *12*(2), 545-554. doi:10.1038/s41385-018-0115-3
- 827 Lasarte, S., Samaniego, R., Salinas-Muñoz, L., Guia-Gonzalez, M. A., Weiss, L. A., Mercader, E.,
828 . . . Relloso, M. (2016). Sex Hormones Coordinate Neutrophil Immunity in the Vagina by

- 829 Controlling Chemokine Gradients. *Journal of Infectious Diseases*, 213(3), 476-484.
830 doi:10.1093/infdis/jiv402
- 831 Lee, A. G., Scott, J. M., Fabbri, M. R., Jiang, X., Sojka, D. K., Miller, M. J., . . . Shin, H. (2020).
832 T cell response kinetics determines neuroinfection outcomes during murine HSV infection.
833 *JCI Insight*, 5(5). doi:10.1172/jci.insight.134258
- 834 Lee, A. J., & Ashkar, A. A. (2012). Herpes simplex virus-2 in the genital mucosa: insights into the
835 mucosal host response and vaccine development. *Current Opinion in Infectious Diseases*,
836 25(1), 92-99. doi:10.1097/QCO.0b013e32834e9a56
- 837 Lee, A. J., Chen, B., Chew, M. V., Barra, N. G., Shenouda, M. M., Nham, T., . . . Ashkar, A. A.
838 (2017). Inflammatory monocytes require type I interferon receptor signaling to activate NK
839 cells via IL-18 during a mucosal viral infection. *The Journal of Experimental Medicine*,
840 214(4), 1153-1167. doi:10.1084/jem.20160880
- 841 Leib, D. A., Harrison, T. E., Laslo, K. M., Machalek, M. A., Moorman, N. J., & Virgin, H. W.
842 (1999). Interferons regulate the phenotype of wild-type and mutant herpes simplex viruses
843 in vivo. *The Journal of Experimental Medicine*, 189(4), 663-672.
844 doi:10.1084/jem.189.4.663
- 845 Li, P., Li, M., Lindberg, M. R., Kennett, M. J., Xiong, N., & Wang, Y. (2010). PAD4 is essential
846 for antibacterial innate immunity mediated by neutrophil extracellular traps. *The Journal*
847 *of Experimental Medicine*, 207(9), 1853-1862. doi:10.1084/jem.20100239
- 848 Li, S., Herrera, G. G., Tam, K. K., Lizarraga, J. S., Beedle, M.-T., & Winuthayanon, W. (2018).
849 Estrogen Action in the Epithelial Cells of the Mouse Vagina Regulates Neutrophil
850 Infiltration and Vaginal Tissue Integrity. *Scientific Reports*, 8(1), 11247.
851 doi:10.1038/s41598-018-29423-5

- 852 Liberzon, A., Birger, C., Thorvaldsdóttir, H., Ghandi, M., Mesirov, J. P., & Tamayo, P. (2015).
853 The Molecular Signatures Database (MSigDB) hallmark gene set collection. *Cell systems*,
854 *1*(6), 417-425. doi:10.1016/j.cels.2015.12.004
- 855 Lijek, R. S., Helble, J. D., Olive, A. J., Seiger, K. W., & Starnbach, M. N. (2018). Pathology after
856 *Chlamydia trachomatis* infection is driven by nonprotective immune cells that
857 are distinct from protective populations. *Proceedings of the National Academy of Sciences*,
858 *115*(9), 2216-2221. doi:10.1073/pnas.1711356115
- 859 Lin, Y., & Zheng, C. (2019). A Tug of War: DNA-Sensing Antiviral Innate Immunity and Herpes
860 Simplex Virus Type I Infection. *Frontiers in Microbiology*, *10*, 2627-2627.
861 doi:10.3389/fmicb.2019.02627
- 862 Luker, G. D., Prior, J. L., Song, J., Pica, C. M., & Leib, D. A. (2003). Bioluminescence imaging
863 reveals systemic dissemination of herpes simplex virus type 1 in the absence of interferon
864 receptors. *Journal of Virology*, *77*(20), 11082-11093. doi:10.1128/jvi.77.20.11082-
865 11093.2003
- 866 Mahlaköiv, T., Hernandez, P., Gronke, K., Diefenbach, A., & Staeheli, P. (2015). Leukocyte-
867 Derived IFN- α/β and Epithelial IFN- λ Constitute a Compartmentalized Mucosal Defense
868 System that Restricts Enteric Virus Infections. *PLOS Pathogens*, *11*(4), e1004782.
869 doi:10.1371/journal.ppat.1004782
- 870 Majer, O., Bourgeois, C., Zwolanek, F., Lassnig, C., Kerjaschki, D., Mack, M., . . . Kuchler, K.
871 (2012). Type I Interferons Promote Fatal Immunopathology by Regulating Inflammatory
872 Monocytes and Neutrophils during *Candida* Infections. *PLOS Pathogens*, *8*(7), e1002811.
873 doi:10.1371/journal.ppat.1002811

- 874 Maruzuru, Y., Ichinohe, T., Sato, R., Miyake, K., Okano, T., Suzuki, T., . . . Kawaguchi, Y. (2018).
875 Herpes Simplex Virus 1 VP22 Inhibits AIM2-Dependent Inflammasome Activation to
876 Enable Efficient Viral Replication. *Cell Host & Microbe*, 23(2), 254-265.e257.
877 doi:<https://doi.org/10.1016/j.chom.2017.12.014>
- 878 Masson, L., Mlisana, K., Little, F., Werner, L., Mkhize, N. N., Ronacher, K., . . . Passmore, J.-A.
879 S. (2014). Defining genital tract cytokine signatures of sexually transmitted infections and
880 bacterial vaginosis in women at high risk of HIV infection: a cross-sectional study.
881 *Sexually transmitted infections*, 90(8), 580-587. doi:10.1136/sextrans-2014-051601
- 882 Mayadas, T. N., Cullere, X., & Lowell, C. A. (2014). The multifaceted functions of neutrophils.
883 *Annual review of pathology*, 9, 181-218. doi:10.1146/annurev-pathol-020712-164023
- 884 Meier, A., Chang, J. J., Chan, E. S., Pollard, R. B., Sidhu, H. K., Kulkarni, S., . . . Altfeld, M.
885 (2009). Sex differences in the Toll-like receptor-mediated response of plasmacytoid
886 dendritic cells to HIV-1. *Nature Medicine*, 15(8), 955-959. doi:10.1038/nm.2004
- 887 Melroe, G. T., DeLuca, N. A., & Knipe, D. M. (2004). Herpes Simplex Virus 1 Has Multiple
888 Mechanisms for Blocking Virus-Induced Interferon Production. *Journal of Virology*,
889 78(16), 8411-8420. doi:10.1128/jvi.78.16.8411-8420.2004
- 890 Milligan, G. N. (1999). Neutrophils Aid in Protection of the Vaginal Mucosae of Immune Mice
891 against Challenge with Herpes Simplex Virus Type 2. *Journal of Virology*, 73(8), 6380-
892 6386. Retrieved from <http://www.ncbi.nlm.nih.gov/pmc/articles/PMC112717/>
- 893 Milligan, G. N., & Bernstein, D. I. (1997). Interferon- γ Enhances Resolution of Herpes Simplex
894 Virus Type 2 Infection of the Murine Genital Tract. *Virology*, 229(1), 259-268.
895 doi:<https://doi.org/10.1006/viro.1997.8441>

- 896 Milligan, G. N., Bourne, N., & Dudley, K. L. (2001). Role of polymorphonuclear leukocytes in
897 resolution of HSV-2 infection of the mouse vagina. *Journal of Reproductive Immunology*,
898 49(1), 49-65. doi:[https://doi.org/10.1016/S0165-0378\(00\)00080-2](https://doi.org/10.1016/S0165-0378(00)00080-2)
- 899 Mittal, M., Siddiqui, M. R., Tran, K., Reddy, S. P., & Malik, A. B. (2014). Reactive Oxygen
900 Species in Inflammation and Tissue Injury. *Antioxidants & Redox Signaling*, 20(7), 1126-
901 1167. doi:10.1089/ars.2012.5149
- 902 Murphy, K., & Mitchell, C. M. (2016). The Interplay of Host Immunity, Environment and the Risk
903 of Bacterial Vaginosis and Associated Reproductive Health Outcomes. *The Journal of*
904 *Infectious Diseases*, 214 Suppl 1(Suppl 1), S29-S35. doi:10.1093/infdis/jiw140
- 905 Nakanishi, Y., Lu, B., Gerard, C., & Iwasaki, A. (2009). CD8(+) T lymphocyte mobilization to
906 virus-infected tissue requires CD4(+) T-cell help. *Nature*, 462(7272), 510-513.
907 doi:10.1038/nature08511
- 908 Narasaraju, T., Yang, E., Samy, R. P., Ng, H. H., Poh, W. P., Liew, A.-A., . . . Chow, V. T. (2011).
909 Excessive neutrophils and neutrophil extracellular traps contribute to acute lung injury of
910 influenza pneumonitis. *The American Journal of Pathology*, 179(1), 199-210.
911 doi:10.1016/j.ajpath.2011.03.013
- 912 Nice, T. J., Osborne, L. C., Tomov, V. T., Artis, D., Wherry, E. J., & Virgin, H. W. (2016). Type
913 I Interferon Receptor Deficiency in Dendritic Cells Facilitates Systemic Murine Norovirus
914 Persistence Despite Enhanced Adaptive Immunity. *PLOS Pathogens*, 12(6), e1005684-
915 e1005684. doi:10.1371/journal.ppat.1005684
- 916 Nowarski, R., Jackson, R., Gagliani, N., de Zoete, Marcel R., Palm, Noah W., Bailis, W., . . .
917 Flavell, Richard A. (2015). Epithelial IL-18 Equilibrium Controls Barrier Function in
918 Colitis. *Cell*, 163(6), 1444-1456. doi:<https://doi.org/10.1016/j.cell.2015.10.072>

- 919 Peng, T., Zhu, J., Klock, A., Phasouk, K., Huang, M.-L., Koelle, D. M., . . . Corey, L. (2009).
920 Evasion of the Mucosal Innate Immune System by Herpes Simplex Virus Type 2. *J. Virol.*,
921 *83*(23), 12559-12568. doi:10.1128/jvi.00939-09
- 922 Pham, C. T. N. (2006). Neutrophil serine proteases: specific regulators of inflammation. *Nat Rev*
923 *Immunol*, *6*(7), 541-550. Retrieved from <http://dx.doi.org/10.1038/nri1841>
- 924 Pylaeva, E., Bordbari, S., Spyra, I., Decker, A. S., Häussler, S., Vybornov, V., . . . Jablonska, J.
925 (2019). Detrimental Effect of Type I IFNs During Acute Lung Infection With
926 *Pseudomonas aeruginosa* Is Mediated Through the Stimulation of Neutrophil NETosis.
927 *Frontiers in Immunology*, *10*(2190). doi:10.3389/fimmu.2019.02190
- 928 Rao, P., & Suvas, S. (2018). Development of Inflammatory Hypoxia and Prevalence of Glycolytic
929 Metabolism in Progressing Herpes Stromal Keratitis Lesions. *The Journal of Immunology*,
930 *ji1800422*. doi:10.4049/jimmunol.1800422
- 931 Reading, P. C., Whitney, P. G., Barr, D. P., Wojtasiak, M., Mintern, J. D., Waithman, J., & Brooks,
932 A. G. (2007). IL-18, but not IL-12, Regulates NK Cell Activity following Intranasal Herpes
933 Simplex Virus Type 1 Infection. *The Journal of Immunology*, *179*(5), 3214-3221.
934 doi:10.4049/jimmunol.179.5.3214
- 935 Reinert, L. S., Harder, L., Holm, C. K., Iversen, M. B., Horan, K. A., Dagnæs-Hansen, F., . . .
936 Paludan, S. r. R. (2012). TLR3 deficiency renders astrocytes permissive to herpes simplex
937 virus infection and facilitates establishment of CNS infection in mice. *The Journal of*
938 *Clinical Investigation*, *122*(4), 1368-1376. Retrieved from
939 <http://www.jci.org/articles/view/60893>

- 940 Robertson, S. E., Young, J. D., Kitson, S., Pitt, A., Evans, J., Roes, J., . . . McInnes, I. B. (2006).
941 Expression and alternative processing of IL-18 in human neutrophils. *European Journal of*
942 *Immunology*, 36(3), 722-731. doi:10.1002/eji.200535402
- 943 Rocha, Bruno C., Marques, Pedro E., Leoratti, Fabiana Maria de S., Junqueira, C., Pereira,
944 Dhelio B., Antonelli, Lis Ribeiro do V., . . . Gazzinelli, Ricardo T. (2015). Type I
945 Interferon Transcriptional Signature in Neutrophils and Low-Density Granulocytes Are
946 Associated with Tissue Damage in Malaria. *Cell Reports*, 13(12), 2829-2841.
947 doi:10.1016/j.celrep.2015.11.055
- 948 Rotger, M., Dang, K. K., Fellay, J., Heinzen, E. L., Feng, S., Descombes, P., . . . Center for, H. I.
949 V. A. V. I. (2010). Genome-wide mRNA expression correlates of viral control in CD4+ T-
950 cells from HIV-1-infected individuals. *PLOS Pathogens*, 6(2), e1000781-e1000781.
951 doi:10.1371/journal.ppat.1000781
- 952 Roychoudhury, P., Swan, D. A., Duke, E. R., Corey, L., Zhu, J., Davé, V. A., . . . Schiffer, J. T.
953 (2020). Tissue-resident T cell derived cytokines eliminate herpes simplex virus-2 infected
954 cells. *The Journal of Clinical Investigation*. doi:10.1172/JCI132583
- 955 Royer, D. J., Hendrix, J. F., Larabee, C. M., Reagan, A. M., Sjoelund, V. H., Robertson, D. M., &
956 Carr, D. J. J. (2019). Vaccine-induced antibodies target sequestered viral antigens to
957 prevent ocular HSV-1 pathogenesis, preserve vision, and preempt productive neuronal
958 infection. *Mucosal immunology*, 12(3), 827-839. doi:10.1038/s41385-019-0131-y
- 959 Saitoh, T., Komano, J., Saitoh, Y., Misawa, T., Takahama, M., Kozaki, T., . . . Akira, S. (2012).
960 Neutrophil Extracellular Traps Mediate a Host Defense Response to Human
961 Immunodeficiency Virus-1. *Cell Host & Microbe*, 12(1), 109-116.
962 doi:<http://dx.doi.org/10.1016/j.chom.2012.05.015>

- 963 Schiffer, J. T., & Corey, L. (2013). Rapid host immune response and viral dynamics in herpes
964 simplex virus-2 infection. *Nature Medicine*, *19*(3), 280-290. doi:10.1038/nm.3103
- 965 Schiffer, J. T., Swan, D., Sallaq, R. A., Magaret, A., Johnston, C., Mark, K. E., . . . Corey, L.
966 (2013). Rapid localized spread and immunologic containment define Herpes simplex virus-
967 2 reactivation in the human genital tract. *eLife*, *2*. doi:10.7554/eLife.00288
- 968 Scott, J. M., Lebratti, T. J., Richner, J. M., Jiang, X., Fernandez, E., Zhao, H., . . . Shin, H. (2018).
969 Cellular and Humoral Immunity Protect against Vaginal Zika Virus Infection in Mice.
970 *Journal of Virology*, *92*(7). doi:10.1128/jvi.00038-18
- 971 Sedaghat, A. R., German, J., Teslovich, T. M., Cofrancesco, J., Jie, C. C., Talbot, C. C., &
972 Siliciano, R. F. (2008). Chronic CD4⁺ T-Cell Activation and Depletion in
973 Human Immunodeficiency Virus Type 1 Infection: Type I Interferon-Mediated Disruption
974 of T-Cell Dynamics. *Journal of Virology*, *82*(4), 1870-1883. doi:10.1128/jvi.02228-07
- 975 Shin, H., & Iwasaki, A. (2013). Generating protective immunity against genital herpes. *Trends in*
976 *Immunology*, *34*(10), 487-494. doi:<http://dx.doi.org/10.1016/j.it.2013.08.001>
- 977 Sommereyns, C., Paul, S., Staeheli, P., & Michiels, T. (2008). IFN-lambda (IFN-lambda) is
978 expressed in a tissue-dependent fashion and primarily acts on epithelial cells in vivo. *PLOS*
979 *Pathogens*, *4*(3), e1000017-e1000017. doi:10.1371/journal.ppat.1000017
- 980 Spang, A. E., Godowski, P. J., & Knipe, D. M. (1983). Characterization of herpes simplex virus 2
981 temperature-sensitive mutants whose lesions map in or near the coding sequences for the
982 major DNA-binding protein. *Journal of Virology*, *45*(1), 332-342. Retrieved from
983 <http://jvi.asm.org/content/45/1/332.abstract>

- 984 Stock, A. T., Smith, J. M., & Carbone, F. R. (2014). Type I IFN suppresses Cxcr2 driven neutrophil
985 recruitment into the sensory ganglia during viral infection. *The Journal of Experimental*
986 *Medicine*. doi:10.1084/jem.20132183
- 987 Sugawara, S., Uehara, A., Nochi, T., Yamaguchi, T., Ueda, H., Sugiyama, A., . . . Takada, H.
988 (2001). Neutrophil Proteinase 3-Mediated Induction of Bioactive IL-18 Secretion by
989 Human Oral Epithelial Cells. *The Journal of Immunology*, 167(11), 6568-6575.
990 doi:10.4049/jimmunol.167.11.6568
- 991 Svensson, A., Bellner, L., Magnusson, M., & Eriksson, K. (2007). Role of IFNalpha/beta signaling
992 in the prevention of genital herpes virus type 2 infection. *Journal of Reproductive*
993 *Immunology*, 74(1,Äi2), 114-123. doi:<http://dx.doi.org/10.1016/j.jri.2006.09.002>
- 994 Swiecki, M., Wang, Y., Gilfillan, S., & Colonna, M. (2013). Plasmacytoid Dendritic Cells
995 Contribute to Systemic but Not Local Antiviral Responses to HSV Infections. *PLOS*
996 *Pathogens*, 9(10), e1003728. doi:10.1371/journal.ppat.1003728
- 997 Taleb, K., Auffray, C., Villefroy, P., Pereira, A., Hosmalin, A., Gaudry, M., & Le Bon, A. (2017).
998 Chronic Type I IFN Is Sufficient To Promote Immunosuppression through Accumulation
999 of Myeloid-Derived Suppressor Cells. *The Journal of Immunology*, 198(3), 1156-1163.
1000 doi:10.4049/jimmunol.1502638
- 1001 Tate, M. D., Deng, Y.-M., Jones, J. E., Anderson, G. P., Brooks, A. G., & Reading, P. C. (2009).
1002 Neutrophils Ameliorate Lung Injury and the Development of Severe Disease during
1003 Influenza Infection. *The Journal of Immunology*, 183(11), 7441-7450.
1004 doi:10.4049/jimmunol.0902497

- 1005 Tate, M. D., Ioannidis, L. J., Croker, B., Brown, L. E., Brooks, A. G., & Reading, P. C. (2011).
1006 The role of neutrophils during mild and severe influenza virus infections of mice. *PLoS*
1007 *ONE*, *6*(3), e17618-e17618. doi:10.1371/journal.pone.0017618
- 1008 Tecchio, C., Micheletti, A., & Cassatella, M. A. (2014). Neutrophil-derived cytokines: facts
1009 beyond expression. *Frontiers in Immunology*, *5*, 508-508. doi:10.3389/fimmu.2014.00508
- 1010 Teijaro, J. R., Ng, C., Lee, A. M., Sullivan, B. M., Sheehan, K. C. F., Welch, M., . . . Oldstone, M.
1011 B. A. (2013). Persistent LCMV Infection Is Controlled by Blockade of Type I Interferon
1012 Signaling. *Science*, *340*(6129), 207-211. doi:10.1126/science.1235214
- 1013 Thomas, J., Gangappa, S., Kanangat, S., & Rouse, B. T. (1997). On the essential involvement of
1014 neutrophils in the immunopathologic disease: herpetic stromal keratitis. *The Journal of*
1015 *Immunology*, *158*(3), 1383-1391. Retrieved from
1016 <https://www.jimmunol.org/content/jimmunol/158/3/1383.full.pdf>
- 1017 Truong, N. R., Smith, J. B., Sandgren, K. J., & Cunningham, A. L. (2019). Mechanisms of Immune
1018 Control of Mucosal HSV Infection: A Guide to Rational Vaccine Design. *Frontiers in*
1019 *Immunology*, *10*(373). doi:10.3389/fimmu.2019.00373
- 1020 Uriarte, S. M., Edmisson, J. S., & Jimenez-Flores, E. (2016). Human neutrophils and oral
1021 microbiota: a constant tug-of-war between a harmonious and a discordant coexistence.
1022 *Immunological Reviews*, *273*(1), 282-298. doi:10.1111/imr.12451
- 1023 Vidy, A., Maisonnasse, P., Da Costa, B., Delmas, B., Chevalier, C., & Le Goffic, R. (2016). The
1024 Influenza Virus Protein PB1-F2 Increases Viral Pathogenesis through Neutrophil
1025 Recruitment and NK Cells Inhibition. *PLoS ONE*, *11*(10), e0165361-e0165361.
1026 doi:10.1371/journal.pone.0165361

- 1027 Wald, A., Zeh, J., Selke, S., Warren, T., Ashley, R., & Corey, L. (2002). Genital Shedding of
1028 Herpes Simplex Virus among Men. *The Journal of Infectious Diseases*,
1029 *186*(Supplement_1), S34-S39. doi:10.1086/342969
- 1030 Wang, J. P., Bowen, G. N., Zhou, S., Cerny, A., Zacharia, A., Knipe, D. M., . . . Kurt-Jones, E. A.
1031 (2012). Role of Specific Innate Immune Responses in Herpes Simplex Virus Infection of
1032 the Central Nervous System. *Journal of Virology*, *86*(4), 2273-2281.
1033 doi:10.1128/jvi.06010-11
- 1034 Wilcox, D. R., Folmsbee, S. S., Muller, W. J., & Longnecker, R. (2016). The Type I Interferon
1035 Response Determines Differences in Choroid Plexus Susceptibility between Newborns and
1036 Adults in Herpes Simplex Virus Encephalitis. *mBio*, *7*(2). doi:10.1128/mBio.00437-16
- 1037 Williams, L. E., Nesburn, A. B., & Kaufman, H. E. (1965). Experimental Induction of Disciform
1038 Keratitis. *JAMA Ophthalmology*, *73*(1), 112-114.
1039 doi:10.1001/archopht.1965.00970030114023
- 1040 Wilson, E. B., Yamada, D. H., Elsaesser, H., Herskovitz, J., Deng, J., Cheng, G., . . . Brooks, D.
1041 G. (2013). Blockade of Chronic Type I Interferon Signaling to Control Persistent LCMV
1042 Infection. *Science*, *340*(6129), 202-207. doi:10.1126/science.1235208
- 1043 Wira, C. R., Rodriguez-Garcia, M., & Patel, M. V. (2015). The role of sex hormones in immune
1044 protection of the female reproductive tract. *Nat Rev Immunol*, *15*(4), 217-230.
1045 doi:10.1038/nri3819
- 1046 World Health Organization, D. o. R. H. a. R. (2007). *Global strategy for the prevention and control*
1047 *of sexually transmitted infections: 2006-2015. Breaking the chain of transmission.*
- 1048 Xin, L., Vargas-Inchaustegui, D. A., Raimer, S. S., Kelly, B. C., Hu, J., Zhu, L., . . . Soong, L.
1049 (2010). Type I IFN Receptor Regulates Neutrophil Functions and Innate Immunity to

- 1050 Leishmania Parasites. *The Journal of Immunology*, 184(12), 7047-7056.
- 1051 doi:10.4049/jimmunol.0903273
- 1052 Zheng, G. X. Y., Terry, J. M., Belgrader, P., Ryvkin, P., Bent, Z. W., Wilson, R., . . . Bielas, J. H.
- 1053 (2017). Massively parallel digital transcriptional profiling of single cells. *Nature*
- 1054 *Communications*, 8(1), 14049. doi:10.1038/ncomms14049
- 1055 Zhu, Q., & Kanneganti, T.-D. (2017). Cutting Edge: Distinct Regulatory Mechanisms Control
- 1056 Proinflammatory Cytokines IL-18 and IL-1 β . *The Journal of Immunology*, 198(11), 4210-
- 1057 4215. doi:10.4049/jimmunol.1700352
- 1058

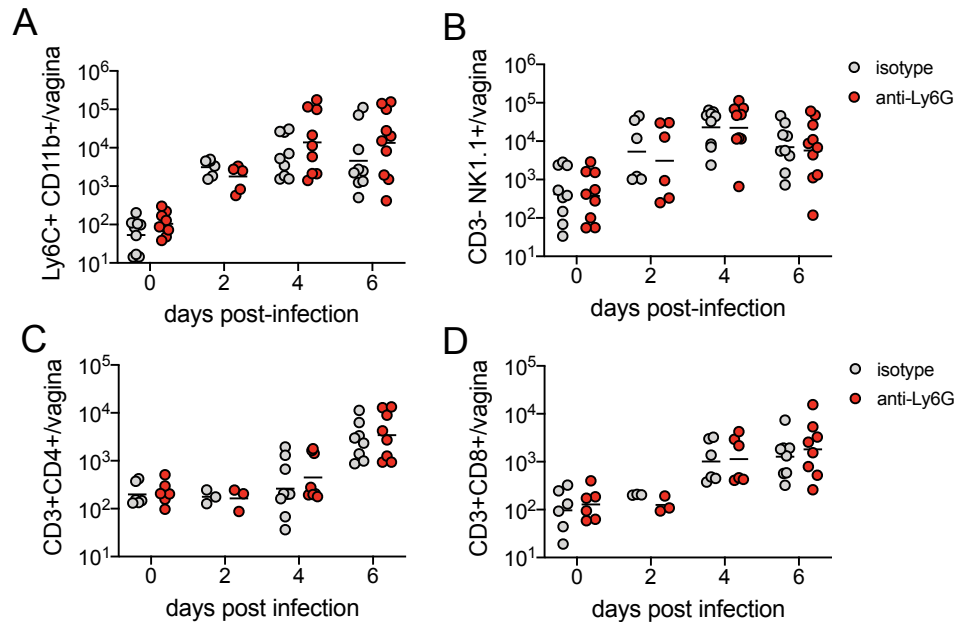


Figure 1 - Supplement 1. Neutrophil depletion does not affect magnitude of the immune cell response after HSV-2 infection. Mice were infected and treated as described in Figure 2. **A-D.** On the indicated d.p.i., immune cell infiltrates were measured in the vagina by flow cytometry. Ly6C+CD11b+ monocytes (**A**), CD3-NK1.1+ NK cells (**B**), CD3+CD4+ T cells (**C**) and CD3+CD8+ T cells (**D**) were enumerated in perfused tissue. (**A, B**) Isotype controls: n=6-9, anti-Ly6G: n=6-10. (**C, D**) Isotype controls: n=3-8, anti-Ly6G: n=3-9. All data are pooled from 2 independent experiments. Horizontal bars show mean (**A-D**). Statistical analysis was performed by two-way ANOVA with Bonferroni's multiple comparisons test. All comparisons were not significant. Raw values for each biological replicate, epsilon values and specific p values are provided in Figure 1 - Supplement 1 source data.

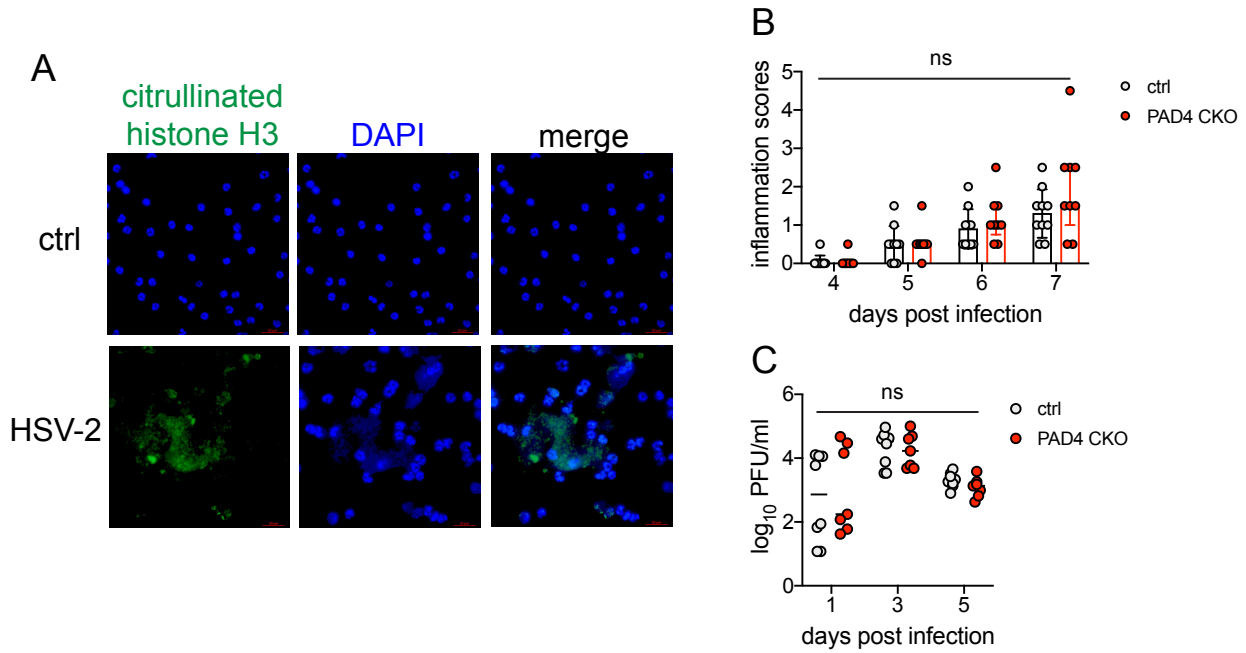


Figure 1 - Supplement 2. PAD4 is not required for development of genital inflammation during HSV-2 infection. **A.** Neutrophils were isolated from the bone marrow of naive C57BL/6 female mice and stimulated with heat-killed HSV-2 at an MOI of 1 for 4 hours (bottom row) or left unstimulated (top row). NETs are identified by areas of diffuse DAPI staining (blue) that overlap with citrullinated histone H3 (green). Data are representative of 2 independent experiments. **B-C.** Pad4^{fl/fl} x MRP8-Cre (PAD4 CKO) or Cre- littermate controls were infected with HSV-2 as described in Figure 1. Inflammation scores were monitored for 7 d.p.i. (Ctrl: n=10, KO: n=9) (**B**), and infectious virus was measured by plaque assay in vaginal washes collected on the indicated d.p.i. (Ctrl: n=8, CKO: n=8) (**C**). Data in **B-C** is pooled from 2 independent experiments. Statistical significance was analyzed by repeated measures two-way ANOVA with (**B**) or without (**C**) Geisser-Greenhouse correction and Bonferroni's multiple comparisons test, ns = not significant. Raw values for each biological replicate, epsilon values and specific p values are provided in Figure 1 - Supplement 2 source data.

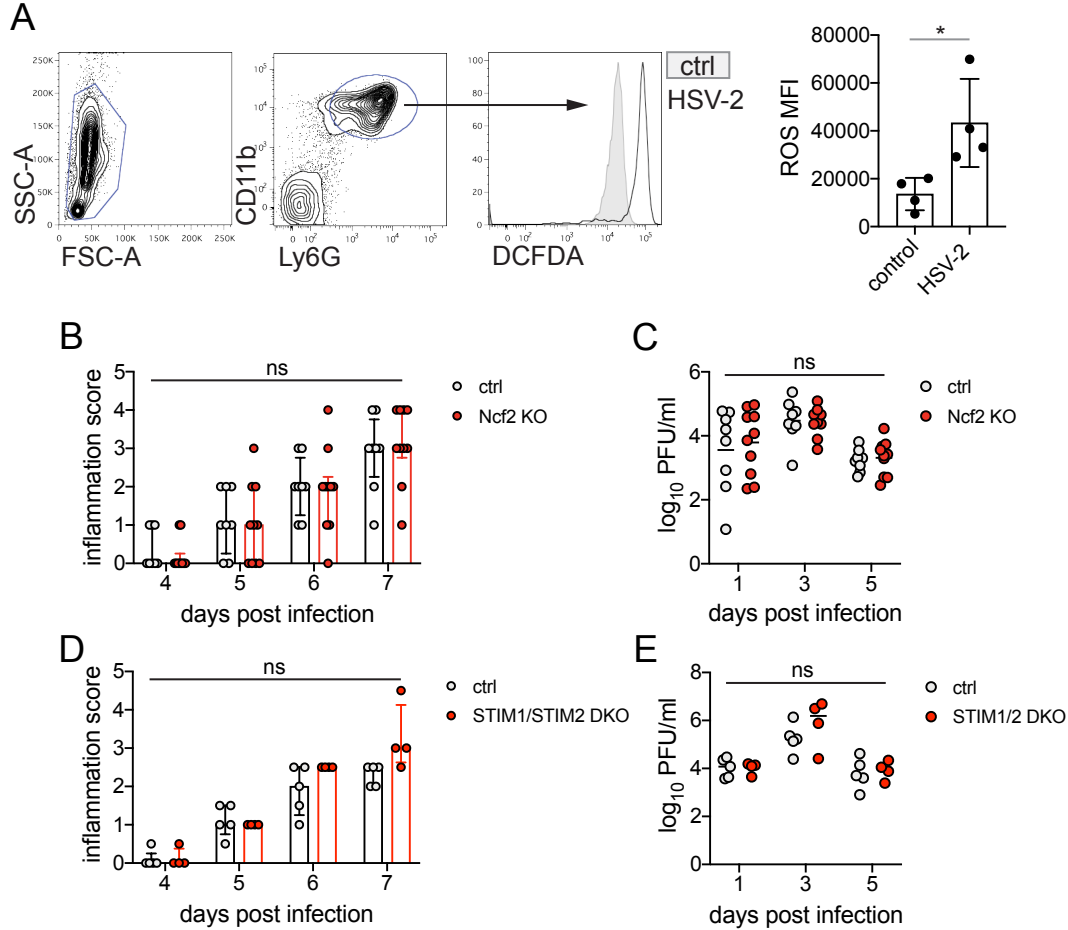


Figure 1 - Supplement 3. ROS production and STIM1/STIM2 expression in neutrophils are not required for genital inflammation after HSV-2 infection. **A.** Neutrophils were isolated from the bone marrow as using a Histopaque gradient and stimulated with heat-killed HSV-2 at an MOI of 5 for 16 hours (n=4) of left unstimulated (n=4) and then incubated with DCFDA. Plots show gating for leukocytes (left) and CD11b+ Ly6G+ neutrophils (middle). DCFDA fluorescence was measured by flow cytometry in unstimulated (shaded histogram) or HSV-2 stimulated (open histogram) neutrophils. Graph shows mean fluorescence intensity (MFI) of DCFDA (ROS). Ncf2 deficient mice (n=10) or littermate controls (n=8) (**B-C**) or STIM1/STIM2 deficient mice (STIM1/STIM2 DKO, n=4) or littermate controls (n=5) (**D-E**) were infected as described in Figure 1. Mice were monitored for genital inflammation for one week after infection (**B, D**). Infectious virus was measured by plaque assay in vaginal washes collected on the indicated days (**C, E**). Bars in **A** show mean with SD. Bars in **B** and **D** show median with interquartile range. Bars in **C** and **E** show mean. Data in **A-C** are pooled from 2 independent experiments, data in **D-E** was performed once. Statistical significance was analyzed by unpaired Student's t-test (**A**), repeated measured two-way ANOVA with (**B, D**) or without (**C, E**) Geisser-Greenhouse correction and Bonferroni's multiple comparisons test, *p<0.05, ns = not significant. Raw values for each biological replicate, epsilon values and specific p values are provided in Figure 1 - Supplement 3 source data.

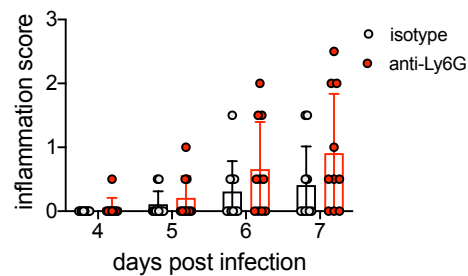


Figure 2 - Supplement 1. Neutrophil depletion prior to HSV-1 genital infection has little impact on disease progression. C57BL/6J females were infected with 10^4 PFU HSV-1 McKrae and treated with neutrophil-depleting antibodies as described in Figure 1. Disease progression was measured during the first 7 d.p.i. for anti-Ly6G (n=10) and isotype control (n=10) mice. Bars show median and interquartile range. Data are pooled from 2 independent experiments. Statistical significance was measured by repeated measured two-way ANOVA with Geisser-Greenhouse correction and Bonferroni's multiple comparisons test. All comparisons were not significant. Raw values for each biological replicate, epsilon values and specific p values are provided in Figure 2 - Supplement 1 source data.

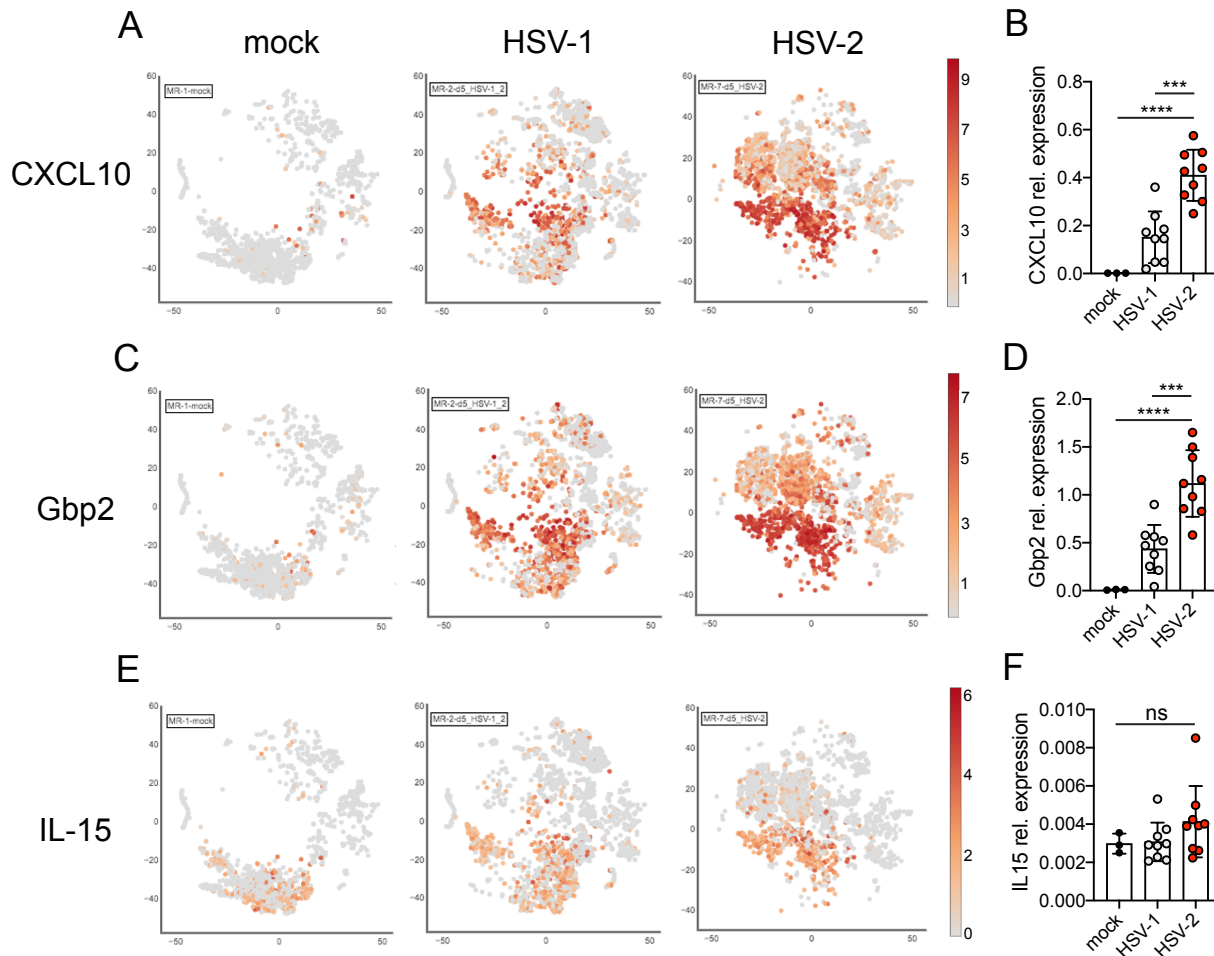


Figure 3 - Supplement 1. Validation of ISG expression in the vagina. Expression of CXCL10 (A, B), Gbp2 (C, D) or IL-15 (E, F) in the vagina of mock inoculated mice or mice at 5 d.p.i. with HSV-1 or HSV-2. tSNE visualization of select ISG transcripts in live vaginal cells profiled by single cell RNA-seq (A, C, E). Expression of the same ISGs relative to Rpl13 was measured by qRT-PCR in whole vaginal tissue harvested from mock inoculated mice (n=3) or mice at 5 d.p.i. with HSV-1 (n=9) or HSV-2 (n=9) (B, D, F). Bars in B, D and F show mean and SD. Data are pooled from 2 independent experiments. Statistical significance was measured by one-way ANOVA with Tukey's multiple comparisons test. ***p<0.005, ****p<0.001, ns = not significant. Raw values for each biological replicate and specific p values are provided in Figure 3 - Supplement 1 source data.

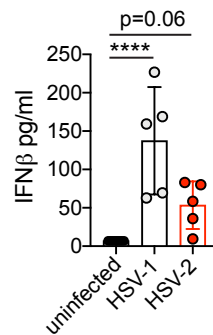


Figure 3 - Supplement 2. Type I IFN is robustly produced in the vagina early after acute HSV-1 or HSV-2 infection. C57BL/6J mice were infected as described in Figure 2. Type I IFN was measured by ELISA in vaginal washes collected from uninfected mice (n=10), or mice at 2 d.p.i. with HSV-1 (n=5) or HSV-2 (n=5). Bars show mean with SD. Experiment was performed once. Statistical significance was measured by one-way ANOVA with Dunnett's multiple comparisons test. ****p<0.001. Raw values for each biological replicate, epsilon values and specific p values are provided in Figure 3 - Supplement 2 source data.

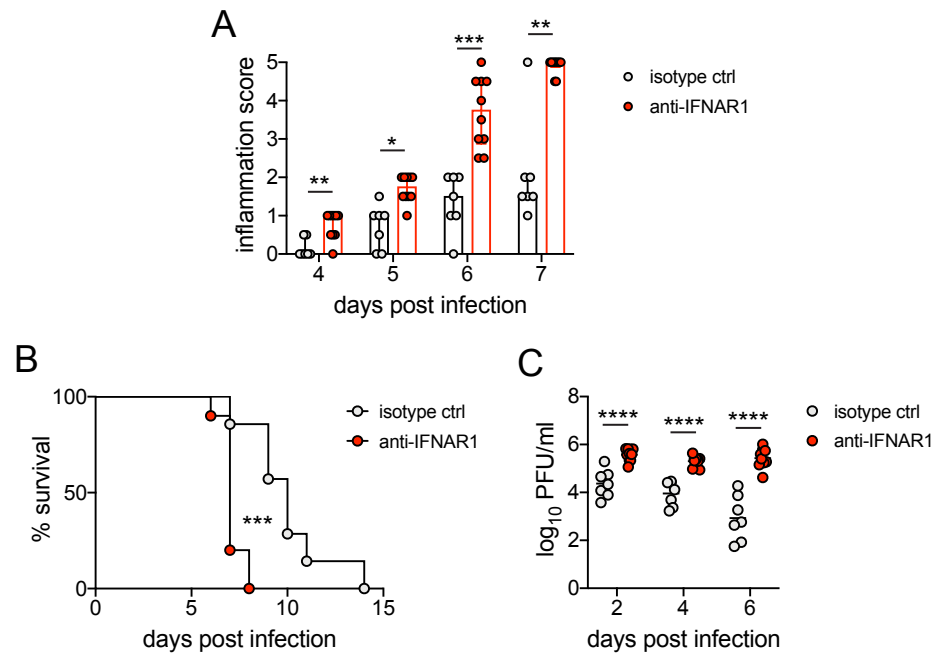


Figure 4 - Supplement 1. Early blockade of IFNAR1 leads to accelerated and more severe disease after HSV-2 infection. C57BL/6J mice were infected as described in Figure 1. On the day of inoculation, mice were injected i.p. with 1mg anti-IFNAR1 antibody (n=10) or an isotype control (n=7). **A.** Inflammation scores of anti-IFNAR antibody or isotype control treated mice for the first 7 d.p.i. **B.** Survival of mice over the course of two weeks. **C.** Infectious virus as measured by plaque assay in vaginal washes collected at the indicated d.p.i.. Bars in **A** show median and interquartile range, bars in **C** show mean. Data are pooled from 3 independent experiments. Statistical significance was measured by repeated measured two-way ANOVA with Geisser-Greenhouse correction and Bonferroni's multiple comparisons test (**A**), log-rank test (**B**) and mixed-effects analysis with Bonferroni's multiple comparisons test (**C**). *p<0.05, **p<0.01, ***p<0.005, ****p<0.001. Raw values for each biological replicate, epsilon values and specific p values are provided in Figure 4 - Supplement 1 source data.

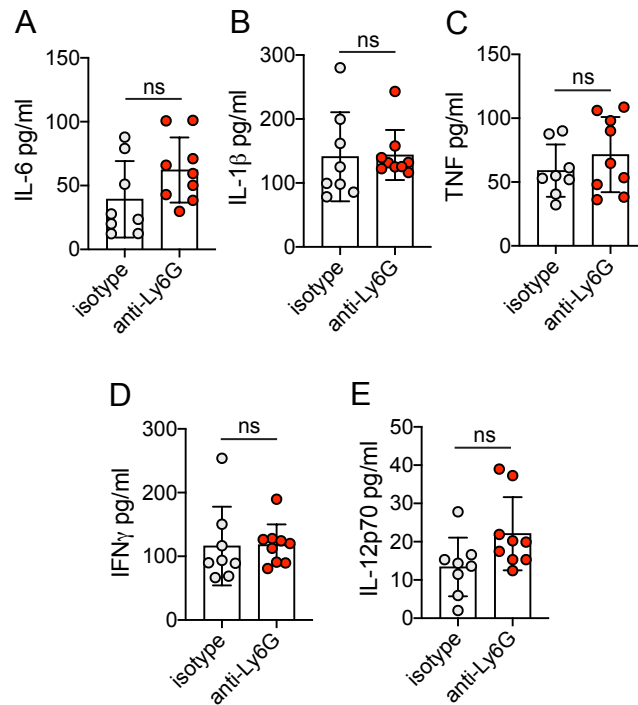


Figure 6 - Supplement 1. Neutrophils do not control production of common pro-inflammatory and antiviral cytokines during HSV-2 infection. Vaginal washes were collected at 5 d.p.i. from mice that were infected and treated as described in Figure 1. IL-6 (A), IL-1b (B), TNF (C), IFN γ (D) and IL-12p70 (E) were measured by multiplexed Bioplex assay. Isotype controls: n=8, anti-Ly6G: n=9. All data are pooled from 2 independent experiments. Statistical analysis was performed by unpaired t-test. ns = not significant. Raw values for each biological replicate and specific p values are provided in Figure 6 - Supplement 1 source data.